Structural and Dynamic Parameters Obtained from ^{17}O NMR, EPR, and NMRD Studies of Monomeric and Dimeric Gd^{3+} Complexes of Interest in Magnetic Resonance Imaging: An Integrated and Theoretically Self-Consistent Approach[1]

D. Hugh Powell,*,†,‡ Orla M. Ni Dhubhghaill,† Dirk Pubanz,† Lothar Helm,† Yakob S. Lebedev,§ Willi Schlaepfer,⊥ and André E. Merbach*,†

Contribution from the Institute of Inorganic and Analytical Chemistry, University of Lausanne, BCH, CH-1015 Lausanne, Switzerland, Department of Chemistry, University of Adelaide, South Australia 5005, Australia, Institute of Chemical Physics, Russian Academy of Sciences, 117977 Moscow V-334, Kosygina 4, Russia, and Institute of Inorganic Chemistry, University of Fribourg, Perolles, CH-1700 Fribourg, Switzerland

Received May 23, 1996[⊗]

Abstract: We present the results of new and previously published ^{17}O NMR, EPR, and NMRD studies of aqueous solutions of the Gd^{3+} octaaqua ion and the commercial MRI contrast agents $[Gd(DTPA)(H_2O)]^{2-}$ (MAGNEVIST, Schering AG, DTPA = 1,1,4,7,7-pentakis(carboxymethyl)-1,4,7-triazaheptane), [Gd(DTPA-BMA)(H_2O)] (OMNISCAN, Sanofi Nycomed, DTPA-BMA = 1,7-bis[(*N*-methylcarbamoyl)methyl]-1,4,7-tris(carboxymethyl)-1,4,7-triazaheptane), and $[Gd(DOTA)(H_2O)]^-$ (DOTAREM, Guerbet, DOTA = 1,4,7,10-tetrakis(carboxymethyl)-1,4,7,10-tetraazacyclododecane). High-field EPR measurements at different concentrations give evidence of an intermolecular dipole−dipole electronic relaxation mechanism that has not previously been described for Gd^{3+} complexes. For the first time, the experimental data from the three techniques for each complex have been treated using a self-consistent theoretical model in a simultaneous multiple parameter least-squares fitting procedure. The lower quality of the fits compared to separate fits of the data for each of the three techniques shows that the increase in the number of adjustable parameters is outweighed by the increased constraint on the fits. The parameters governing the relaxivity of the complexes are thus determined with greater confidence than previously possible. The same approach was used to study two dimeric Gd^{3+} complexes [pip{Gd(DO3A)(H_2O)}$_2$] and [bisoxa{Gd(DO3A)(H_2O)}$_2$] (pip(DO3A)$_2$ = bis(1,4-(1-(carboxymethyl)-1,4,7,10-tetraaza-4,7,10-tris(carboxymethyl)-1-cyclododecyl-1,4-diazacyclohexane, bisoxa-(DO3A)$_2$ = bis(1,4-(1-(carboxymethyl)-1,4,7,10-tetraaza-4,7,10-tris(carboxymethyl)-1-cyclododecyl))-1,10-diaza-3,6-dioxadecane) that are being developed as potential second-generation MRI contrast agents. These dimeric complexes are expected to have higher relaxivities than the monomeric contrast agents, due to their longer rotational correlation times. The results of this study show that further relaxivity gain for these complexes will be hindered by the slow rate of water exchange on the complexes. High-field EPR measurements suggest that there is a previously unrecorded intramolecular dipole−dipole mechanism of electronic relaxation, but that this additional contribution to electronic relaxation is of minor importance compared to the limiting effect of water exchange rates in the determination of proton relaxivity in MRI applications.

Introduction

In medical magnetic resonance imaging (MRI), the intensity of the ^1H NMR signal (due mainly to water protons) is measured for spatially encoded volume elements in the body. The image contrast results primarily from the different relaxation rates of water protons in different tissues. This contrast can be enhanced by paramagnetic ions such as Gd^{3+} that increase the proton relaxation rates in surrounding water.[2] In order to reduce toxicity to an acceptable level, the paramagnetic agent is injected in the form of a stable poly(amino carboxylate) complex. The ability of such a paramagnetic complex to accelerate proton relaxation, its *relaxivity*, is due to the modulation of through-space dipole−dipole interactions between the unpaired electron spin on the paramagnetic ion and the proton nuclei of the surrounding water. This effect is separated for convenience into "inner-sphere" relaxivity due to interactions with water molecules bound in the first coordination sphere of the paramagnetic metal and transferred to the bulk water by chemical exchange and "outer-sphere" relaxivity due to direct interactions with bulk water in the vicinity of the paramagnetic complex.[3] In the Gd complexes currently used as contrast agents, all of which contain one inner-sphere water molecule, the contributions of these two effects are of similar magnitude.[3]

Inner-sphere relaxivity is governed by four characteristic time constants: the correlation time for the rotation of the complex, τ_R , the residence time of a water proton in the inner-coordination sphere, τ_m (often expressed as its inverse, the exchange rate $k_{ex} = 1/\tau_m$), and the longitudinal and transverse electronic relaxation times ($T_{1,2e}$).[2,3] The proton residence time under physiological conditions is normally assumed to be equal to the residence time of the oxygen nucleus since, at neutral pH, proton exchange is expected to take place primarily via

† University of Lausanne.
‡ University of Adelaide.
§ Russian Academy of Sciences.
⊥ University of Fribourg.
⊗ Abstract published in *Advance ACS Abstracts,* September 15, 1996.
(1) Part 74 of the series High-Pressure NMR kinetics. Part 73: Moullet, B.; Zwahlen, C.; Frey, U.; Gervasio, G.; Merbach, A. E. Submitted for publication.
(2) Lauffer, R. B. *Chem. Rev.* **1987**, *87*, 901.
(3) Koenig, S. H.; Brown, R. D., III. *Prog. NMR Spectrosc.* **1990**, *22*, 487.

S0002-7863(96)01743-X CCC: $12.00

the exchange of whole water molecules. This hypothesis was confirmed recently for [Gd(DTPA-BMA)(H_2O)].[4,5] The outer-sphere contribution to relaxivity depends mainly on the electronic relaxation rates and the rate at which an outer-sphere water molecule diffuses away from the gadolinium complex.[3]

New MRI contrast agents must display considerable gains in performance in order to penetrate a highly competitive market. If one is to take a rational, rather than trial-and-error, approach to the design of new drugs, one requires a detailed knowledge of the mechanisms that produce relaxivity, and an understanding of how changes in the chemical structure of the drug interfere with these mechanisms. The first technique to probe these mechanisms in any detail was NMRD (Nuclear Magnetic Resonance Dispersion), where the excess longitudinal proton relaxation caused by the presence of the contrast agent is measured as a function of magnetic field using a field-cycling technique.[3] The method is a direct measure of proton relaxivity, and is in principle sensitive to all the parameters that influence relaxivity. The technique has played a central role in the development of our understanding of proton relaxivity, and in particular showed that there are relaxivity gains to be made by slowing down the rotation of the complexes. This has been the main rationale behind the development of new high molecular weight contrast agents.

A major problem with NMRD studies is that, since there are many parameters that influence the relaxivity, these are often ill-defined by the NMRD curve alone. In particular, the relative contributions from outer- and inner-sphere relaxivity to the NMRD curve cannot be determined for a given complex. The outer-sphere relaxivity is normally either assumed to be equal to that for a similar Gd^{3+} complex known to have no water in the inner-coordination sphere or estimated from reasonable parameters. As has been stressed by one of the pioneers of NMRD an accurate interpretation of NMRD profiles can only be made by reference to independent information from other techniques.[6] A combination of two techniques, EPR and ^{17}O NMR, has proved especially useful as a probe for a number of the parameters of importance to proton relaxivity.[4,7]

EPR line widths give direct access to transverse electronic relaxation rates. Using measurements at multiple magnetic fields and a suitable model, the longitudinal relaxation rates may be calculated[8] (the electronic relaxation of Gd^{3+} is too rapid to allow longitudinal relaxation rates to be determined directly using pulse sequences). The measurement of ^{17}O NMR transverse and longitudinal relaxation rates and chemical shifts over a range of magnetic fields as a function of temperature and pressure permits estimates of the number of inner-sphere water molecules, the rotational correlation time, and the longitudinal electronic relaxation rate of the complexes.[4,9,10] Most importantly, however, the technique allows accurate determinations of the rate of exchange of water between the inner-sphere and bulk water, and variable pressure measurements allow the mechanism of the exchange reaction to be elucidated.[11,12] Contrary to estimates made in the analysis of NMRD profiles, the water exchange rates found for contrast agents by ^{17}O NMR were several orders of magnitude lower than that on the Gd^{3+} aqua ion.[4,9,10] Indeed, in at least one case, the water exchange process was shown to be sufficiently slow to reduce the efficiency of transfer of relaxation from the inner-sphere to the bulk.[4,5] These results suggested that, in the development of new high molecular weight contrast agents, good ligand design would be essential to ensure that slow water exchange rates did not negate a large part of the relaxivity gains expected from a slowing of the rotation of the complexes. Mechanistic studies enabled a rationalization of the observed water exchange rates on the contrast agents, and gave some clues as to how the water exchange rate could be tuned by appropriate ligand design.

Up to now, although the combination of ^{17}O NMR and EPR results has been used to better define certain common parameters,[4,10] they have not been submitted to a true simultaneous analysis. In addition, they have been analyzed in isolation from the results of NMRD experiments. This has been partly due to the paucity of variable-temperature NMRD results available in the literature. Since the results of the three techniques are influenced by a number of common parameters, it would seem more reasonable where possible to subject them to a simultaneous least-squares fitting procedure. This should allow a more reliable determination of the set of parameters governing proton relaxivity, provide a more stringent test of the relaxation theories applied to the three techniques, and permit a validation of current models for the dynamics in paramagnetic solutions.

We present such an integrated analysis of ^{17}O NMR, EPR, and NMRD data for a series of Gd^{3+} complexes that have already been extensively investigated, namely the octaaqua ion $[Gd(H_2O)_8]^{3+}$,[10] and the three commercial MRI contrast agents $[Gd(DTPA)(H_2O)]^{2-}$ (MAGNEVIST, Schering),[9] [Gd(DTPA-BMA)(H_2O)] (OMNISCAN, Sanofi Nycomed),[4] and $[Gd(DOTA)(H_2O)]^-$ (DOTAREM, Guerbet)[9] (see Chart 1 for structural formulas). Although much of the experimental data have already been reported in the literature, we have made additional measurements in order to present a uniform approach to the four complexes. In addition we present a similar integrated approach to new ^{17}O NMR, EPR, and NMRD data for two developmental contrast agents—[pip{Gd(DO3A)-(H_2O)}$_2$] and [bisoxa{Gd(DO3A)(H_2O)}$_2$] (both from Sanofi Nycomed, see Chart 1 for structural formulas). These dimeric Gd^{3+} complexes can be seen as a first step in the development of high molecular weight polymeric contrast agents, the expectation being that they will have longer rotational correlation times and thus higher proton relaxivities than the monomeric complexes. For all the aforementioned complexes we also present new high-field EPR data at a range of concentrations. These data are interpreted in terms of inter- and intramolecular dipole−dipole relaxation mechanisms that have not previously been reported for Gd^{3+} complexes.

Experimental Section

Sample Preparation. All solutions were prepared by weight. The solid gadolinium complexes with the five ligands investigated were provided by Sanofi Nycomed, USA, and used without further purification. They were dissolved in double distilled water and the pH, measured with a combined glass electrode calibrated with Metrohm buffers, was adjusted by adding weighed amounts of aqueous solutions of perchloric acid or sodium hydroxide of known concentration. The absence of free metal was checked by the xylenol orange test.[13] [Gd-(H_2O)$_8$]$^{3+}$ was prepared by dissolving excess gadolinium oxide (NU-

(4) Gonzalez, G.; Powell, D. H.; Tissières, V.; Merbach A. E. *J. Phys. Chem.* **1994**, *98*, 53.
(5) Aime, S.; Botta, M.; Fasano, M.; Paoletti, S.; Anelli, P. M; Uggeri, F.; Virtuani, M. *Inorg. Chem.* **1994**, *33*, 4707.
(6) Koenig, S. H. *J. Magn. Reson.* **1978**, *31*, 1.
(7) Powell, D. H.; Merbach, A. E.; González, G.; Brücher, E.; Micskei, K.; Ottaviani, M. F.; Köhler, K.; von Zelewsky, A.; Grinberg, O. Y.; Lebedev, Ya.S. *Helv. Chim. Acta* **1993**, *76*, 2129.
(8) Reuben, J. *J. Phys. Chem.* **1971**, *75*, 3164.
(9) Micskei, K.; Helm, L.; Brücher, E.; Merbach, A. E. *Inorg. Chem.* **1993**, *32*, 3844.
(10) Micskei, K.; Powell, D. H.; Helm, L.; Brücher, E.; Merbach A. E. *Magn. Reson. Chem.* **1993**, *31*, 1011.
(11) Frey, U.; Merbach, A. E.; Powell, D. H. Solvent Exchange on Metal Ions: A Variable Pressure Approach. In *Dynamics of Solutions and Fluid Mixtures by NMR*; Delpuech, J.-J., Ed.; John Wiley & Sons: New York, 1995.
(12) Lincoln, S. F.; Merbach, A. E. *Adv. Inorg. Chem.* **1995**, *42*, 1.
(13) Brunisholz, G.; Randin, M. *Helv. Chim. Acta* **1959**, *42*, 1927.

Chart 1. Structures of the Different Ligands Referred to in This Study

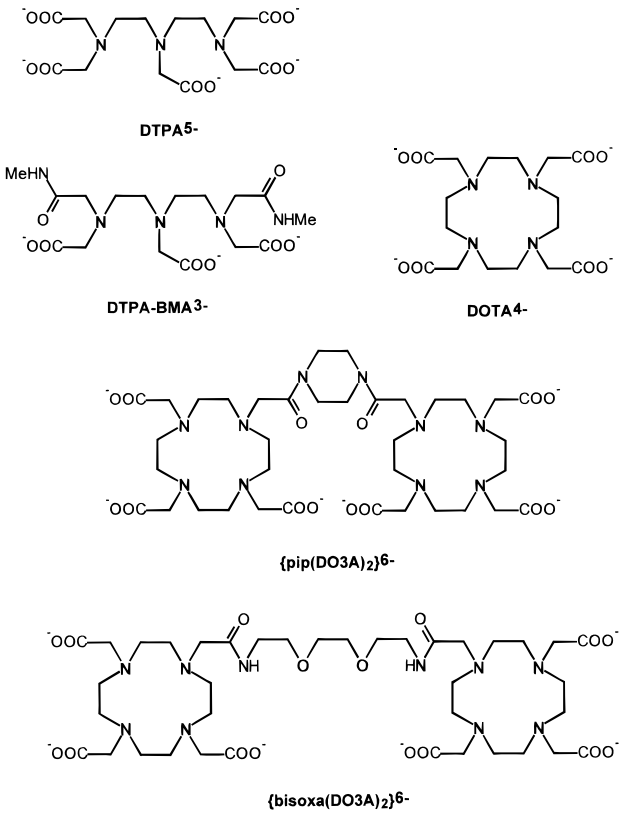

COR Corp., 99.99%) in perchloric acid followed by filtration, and the pH was adjusted as for the other solutions. ^{17}O-enriched water (Yeda R&D Co., Rehovot, Israel) was added to the solutions for the ^{17}O NMR measurements to improve sensitivity and the pH was checked again. The compositions of the different solutions are shown in Table 1.

EPR. The EPR spectra were measured at X-band (Lausanne), Q-band (Fribourg), and 2-mm-band (Moscow). All spectrometers were operated in continuous wave mode. The 2-mm spectrometer in Moscow is home built, the Q- and X-band spectrometers were manufactured by Varian and Bruker, respectively. All measurements at 2-mm band were performed with a semifocal Fabri-Perot resonator. For the 2-mm-band measurements, the samples were contained between two glass plates,[14] and for Q- and X-bands in 0.3- and 1 mm glass tubes, respectively. The acquisition parameters, especially modulation amplitude and microwave power, were varied and the final spectra recorded with values that did not affect the line width. The peak-to-peak line width was measured from the recorded spectrum either with a ruler or using instrument software. The cavity temperature was stabilized using electronic temperature control of gas flowing through the cavity. For the X- and Q-band measurements, the temperature was verified by substituting a thermometer for the sample tube. Measurements were made at temperatures from 273.2 K to the maximum obtainable for each instrument.

^{17}O NMR. Variable-temperature ^{17}O NMR measurements were performed at three different magnetic fields using Bruker AM-400 (9.4 T, 54.2 MHz) and AC-200 (4.7 T, 27.1 MHz), spectrometers and a WP-60 electromagnet (1.4 T, 8.1 MHz) adapted for use with the AC-200 console. Bruker VT-1000 temperature control units were used to stabilize the temperature, which was measured by a substitution technique.[15] The samples were sealed in glass spheres, fitting into 10-mm NMR tubes, in order to eliminate susceptibility corrections to the chemical shift.[16] Longitudinal relaxation rates, $1/T_1$, were obtained by the inversion recovery method,[17] and transverse relaxation rates, $1/T_2$, by the Carr−Purcell−Meiboom−Gill spin echo technique[18] or, for line widths greater than 1 kHz, directly from the line widths. Variable-pressure NMR measurements were performed up to 200 MPa on a Bruker AM-400 spectrometer equipped with a home built probehead.[19] The temperature was then controlled by circulating a fluid from an external temperature bath and measured using a built-in Pt resistor. The transverse relaxation rates were measured as for the variable temperature work.

Table 1. Compositions of the Different Solutions Used in This Study

complex	for method	$[Gd^{3+}]$	pH
$[Gd(H_2O)_8]^{3+}$	EPR	0.0051	1.07
	EPR	0.0100	1.12
	EPR	0.0210	1.10
	EPR	0.0400	1.10
	EPR	0.0600	1.13
	NMR	0.0100	2.00
	NMRD	see ref 3	
$[Gd(DTPA)(H_2O)]^{2-}$	EPR	0.0059	5.3
	EPR	0.0135	5.3
	EPR	0.0251	5.3
	EPR	0.0596	5.3
	EPR	0.170	5.3
	NMR	0.0500	5.3
	NMRD	0.0015	7.2
[Gd(DTPA-BMA)(H_2O)]	EPR	0.0048	4.07
	EPR	0.0150	4.09
	EPR	0.0240	4.03
	EPR	0.0400	4.00
	EPR	0.0520	4.08
	NMR	0.234	4.1
	NMR	0.360	4.1
	NMRD	0.0015	7.2
$[Gd(DOTA)(H_2O)]^{-}$	EPR	0.0060	5.1
	EPR	0.0102	5.1
	EPR	0.0193	5.2
	EPR	0.0519	5.2
	EPR	0.0610	5.0
	NMR	0.0504	5.1
	NMRD	0.00113	5.1
[pip{Gd(DO3A)(H_2O)}$_2$]	EPR	0.0049	4.2
	EPR	0.0080	4.1
	EPR	0.0163	4.2
	EPR	0.0443	4.1
	EPR	0.0686	4.0
	NMR	0.132	3.1
	NMRD	0.0010	7.2
[bisoxa{Gd(DO3A)(H_2O)$_2$}]	EPR	0.0037	3.9
	EPR	0.0083	4.0
	EPR	0.0151	4.1
	EPR	0.0370	4.0
	EPR	0.0751	4.0
	NMR	0.160	3.9
	NMRD	0.0010	7.2

Results

We begin with a presentation of the EPR results, since the treatment of the electronic relaxation rates has consequences for analysis of the two other techniques. We present firstly high-field, variable-temperature and concentration results, which are analyzed separately, followed by the multiple field, variable temperature results, which are analyzed simultaneously with the ^{17}O NMR and NMRD data. We then present the variable temperature ^{17}O NMR and NMRD data, and the simultaneous analysis of the results of the three methods. Finally, we present the results of a variable-pressure ^{17}O NMR study of the mechanism of water exchange on [bisoxa{Gd(DO3A)(H_2O)$_2$}].

(14) Lebedev, Y. S. In *Modern Pulsed and Continuous Wave Electron Spin Resonance*; Kevan, L., Bowman, M., Eds.; Wiley: New York, 1990.
(15) Ammann, C.; Meier, P.; Merbach, A. E. *J. Magn. Reson.* **1982**, *46*, 319.
(16) Hugi, A. D.; Helm, L.; Merbach, A. E. *Helv. Chim. Acta* **1985**, *68*, 508.
(17) Vold, R. V.; Waugh, J. S.; Klein, M. P.; Phelps, D. E. *J. Chem. Phys.* **1968**, *48*, 3831.
(18) Meiboom, S.; Gill, D. *Rev. Sci. Instrum.* **1958**, 29, 688.
(19) Frey, U.; Helm, L.; Merbach, A. E. *High Pressure Res.* **1990**, *2*, 237.

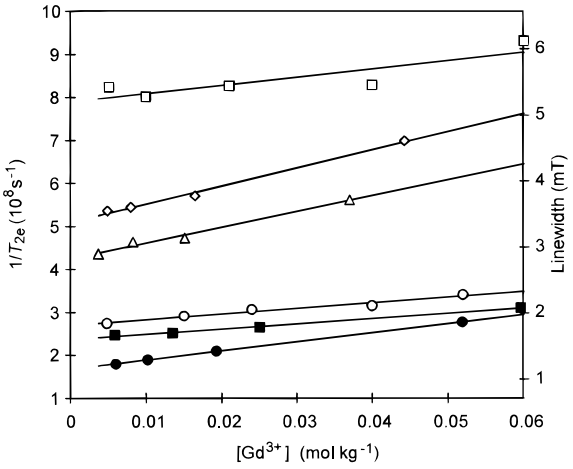

Figure 1. Concentration dependence of the EPR line widths (and transverse electronic relaxation rates) at 5.0 T and 300 K of Gd^{3+} in $[Gd(H_2O)_8]^{3+}$ (□), $[Gd(DTPA)(H_2O)]^{2-}$ (●), [Gd(DTPA-BMA)(H_2O)] (■), $[Gd(DOTA)(H_2O)]^{2-}$ (○), [pip{Gd(DO3A)(H_2O)$_2$}] (◇), and [bisoxa{Gd(DO3A)(H_2O)$_2$}] (△).

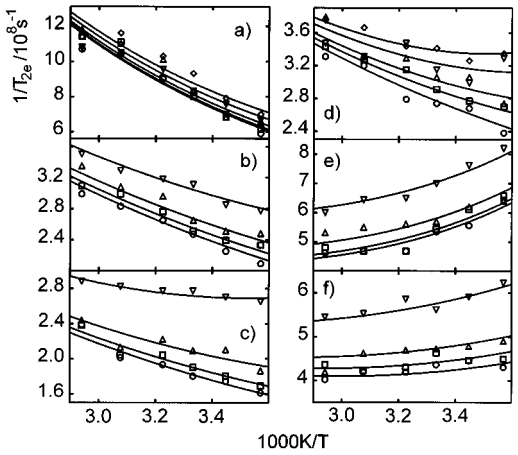

Figure 2. Concentration and temperature dependence of the transverse electronic relaxation rates at 5.0 T of Gd^{3+} in (a) 0.0051 m, 0.01 m, 0.021 m, 0.04 m, and 0.06 m $[Gd(H_2O)_8]^{3+}$, (b) 0.0048 m, 0.015 m, 0.024 m, 0.04 m, and 0.052 m [Gd(DTPA-BMA)(H_2O)], (c) 0.0059 m, 0.0135 m, 0.0251 m, and 0.0596 m $[Gd(DTPA)(H_2O)]^{2-}$, (d) 0.006 m, 0.0102 m, 0.0193 m, and 0.0519 m $[Gd(DOTA)(H_2O)]^{-}$, (e) 0.0049 m, 0.008 m, 0.0163 m, and 0.0443 m [pip{Gd(DO3A)(H_2O)$_2$}], and (f) 0.0037 m, 0.0083 m, 0.0151 m, and 0.037 m [bisoxa{Gd(DO3A)-(H_2O)$_2$}]. The successive symbols ○, □, △, ▽ and ◇ correspond to increasing concentrations. The curves correspond to fits of the data in terms of inter- and intramolecular dipole−dipole relaxation mechanisms as described in the text.

High-Field EPR Measurements—Inter- and Intramolecular Dipole−Dipole Relaxation. The 2-mm-band (5.0 T) EPR line shapes of the six Gd^{3+} complexes were all approximately Lorentzian, and appeared at a field corresponding to a Landé g factor, $g_L = 2.0$ within experimental error. The transverse electronic relaxation rates, $1/T_{2e}$, were calculated from the peak-to-peak EPR line widths, ΔH_{pp}, using eq 1, where the symbols have their usual meaning.[8]

$$\frac{1}{T_{2e}} = \frac{g_L \mu_B \pi \sqrt{3}}{h} \Delta H_{pp} \qquad (1)$$

For all the Gd^{3+} complexes studied, and at all temperatures, the line widths, and hence relaxation rates, increased with increasing solution concentration (see results at 300 K in Figure 1). The concentration dependence, observed systematically for the first time in these new measurements, was linear within error in the range up to 0.06 m. The most likely source of this concentration dependent contribution to the line width is relaxation due to intermolecular dipole−dipole relaxation between Gd^{3+} ions in different complexes. The theory for intermolecular dipole−dipole interaction between unlike spins, modulated by diffusion processes, is widely used to describe proton relaxation in the presence of paramagnetic species:[3,20] this can be modified for like spins following *Abragam*[21] to give eqs 2 and 3 for the electronic relaxation rates, where the spectral

$$\left(\frac{1}{T_{1e}}\right)^{\text{inter}} = [Gd^{3+}] \frac{(3.2 \times 10^3)\pi N_A}{27} \left(\frac{\mu_o}{4\pi}\right)^2 \frac{\hbar^2 \gamma_S^4 S(S+1)}{a_{GdGd} D_{GdGd}} (2J_1^{\text{inter}} + 8J_2^{\text{inter}}) \qquad (2)$$

$$\left(\frac{1}{T_{2e}}\right)^{\text{inter}} = [Gd^{3+}] \frac{(3.2 \times 10^3)\pi N_A}{27} \left(\frac{\mu_o}{4\pi}\right)^2 \frac{\hbar^2 \gamma_S^4 S(S+1)}{a_{GdGd} D_{GdGd}} (3J_0^{\text{inter}} + 5J_1^{\text{inter}} + 2J_2^{\text{inter}}) \qquad (3)$$

density function, J_n^{inter}, is defined by eq 4, where γ_S is the

$$J_n^{\text{inter}} = \text{Re}\left(\left\{1 + \frac{1}{4}\left(in\omega_S\tau_{GdGd} + \frac{\tau_{GdGd}}{T_{je}}\right)^{1/2}\right\} \Big/ \left\{1 + \left(in\omega_S\tau_{GdGd} + \frac{\tau_{GdGd}}{T_{je}}\right)^{1/2} + \frac{4}{9}\left(in\omega_S\tau_{GdGd} + \frac{\tau_{GdGd}}{T_{je}}\right) + \frac{1}{9}\left(in\omega_S\tau_{GdGd} + \frac{\tau_{GdGd}}{T_{je}}\right)^{3/2}\right\}\right) \quad \text{with } j = 1, 2 \qquad (4)$$

electron gyromagnetic ratio ($\gamma_S = g_L\mu_B/\hbar = 1.76 \times 10^{11}$ rad s^{-1} T^{-1} for $g_L = 2.0$), ω_S is the Larmor frequency of the spin S ($S = {}^7/_2$ for Gd^{3+}), T_{je} are the overall electronic relaxation times, a_{GdGd} is the distance of closest approach of two Gd^{3+} ions in different complexes, and D_{GdGd} is the diffusion constant of one complex with respect to another. The correlation time, $\tau_{GdGd} = a_{GdGd}^2/D_{GdGd}$, corresponds to the time taken for two complexes to diffuse apart.

The treatment of this relaxation mechanism is complicated by the fact that both diffusion and the electronic relaxation rates themselves can modulate the dipole−dipole interaction, so that the Redfield limit implicit in the relaxation equations does not strictly apply.[21] However, the deviations will be small provided the diffusional correlation time is much shorter than the electronic relaxation times. Consider the aqua ion $[Gd(H_2O)_8]^{3+}$. The distance of closest approach of two Gd^{3+} ions can be estimated to be twice the Gd−H distance, which can be estimated at 3.05 Å from neutron diffraction data for Sm^{3+} and Nd^{3+} solutions.[22,23] The diffusion coefficient for the $[Gd(H_2O)_8]^{3+}$ should be similar to the limiting value of 6×10^{-10} m^2 s^{-1} at 298 K found for La^{3+} in aqueous $LnCl_3$ solution,[24] and the diffusion coefficient for motion of one complex relative

(20) Freed, J. H. *J. Chem. Phys.* **1978**, *68*, 4034.
(21) Abragam, A. *The Principles of Nuclear Magnetism*; Oxford University Press: London, 1961; pp 289−305.
(22) Cossy, C.; Barnes, A. C.; Enderby, J. E.; Merbach, A. E. *J. Chem. Phys.* **1989**, *90*, 3254.
(23) Cossy, C.; Powell, D. H.; Helm, L.; Merbach, A. E. *New J. Chem.* **1995**, *19*, 27.
(24) Weingärtner, H.; Braun, B. M.; Schmoll, J. M. *J. Phys. Chem.* **1987**, *91*, 979.

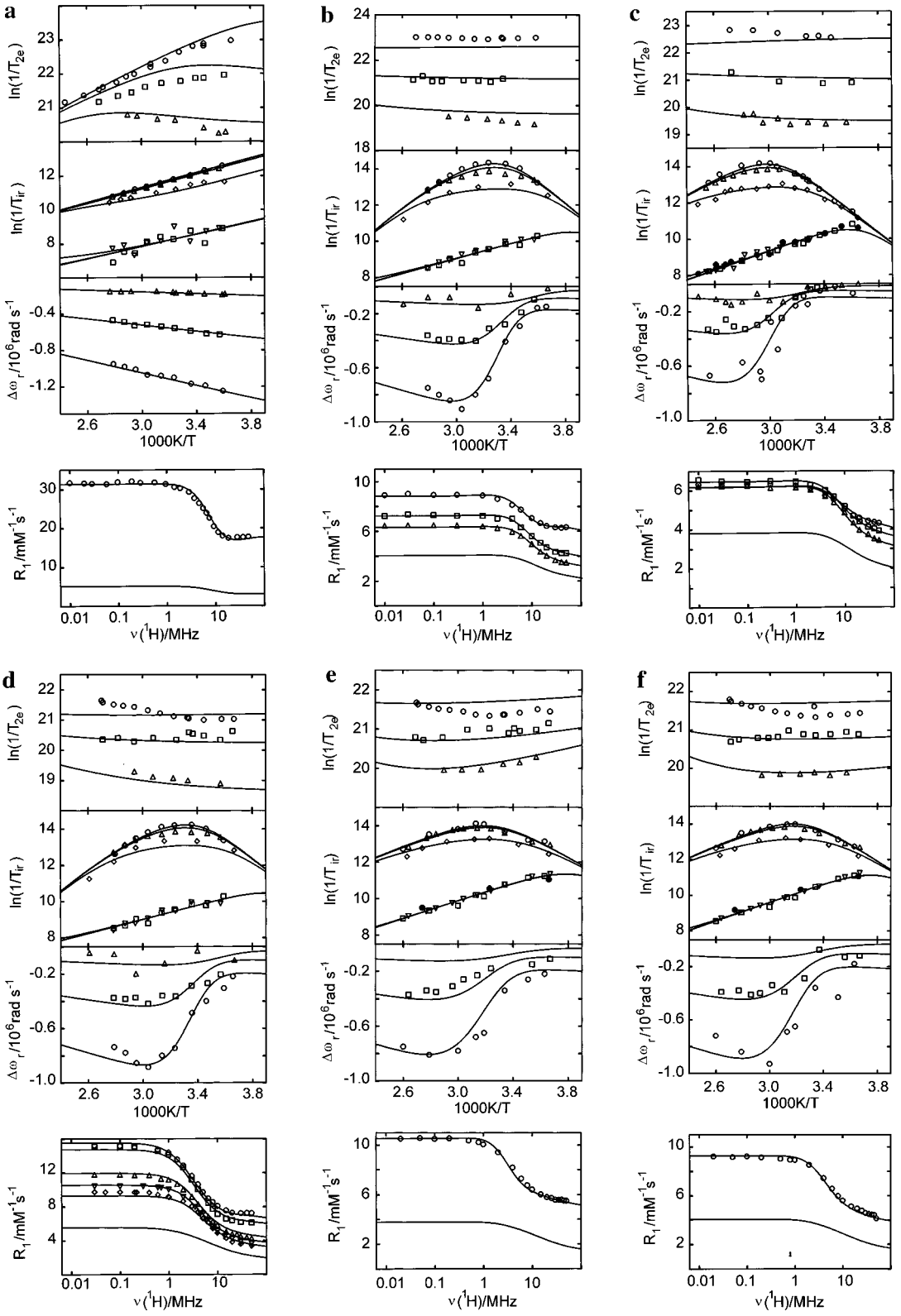

Figure 3. Temperature dependence of transverse electronic relaxation rates (top box) of Gd^{3+}, at X- (0.34 T, ○), Q- (1.2 T, □) and 2-mm- (5.0 T, △) band, of reduced transverse (◇, △, ○) and longtudinal (●, ▽, □) ^{17}O relaxation rates (second box from top) at 1.41, 4.7, and 9.4 T, of reduced ^{17}O chemical shifts (third box from top) at 1.41 (△), 4.7 (□), and 9.4 T (○); NMRD profiles in saline buffer (bottom box) for (a) $[Gd(H_2O)_8]^{3+}$ (NMRD profile at 283.2 K), (b) $[Gd(DTPA)(H_2O)]^{2-}$ (NMRD profiles at 278.2 (○), 298.2 (□), and 308.2 K (△)), (C) [Gd(DTPA-BMA)(H_2O)] (NMRD profiles at 278.2 (○), 298.2 (□), and 308.2 K (△)), (d) $[Gd(DOTA)(H_2O)]^{-}$ (NMRD profiles at 277.2 (○), 283.2 (□), 298.2 (△), 305.2 (▽), 312.2 K (◇)), (e) [pip{Gd(DO3A)(H_2O)}$_2$] (NMRD profile at 309.2 K), and (f) [bisoxa{Gd(DO3A)(H_2O)}$_2$] (NMRD profile at 309.2 K). The lines represent simultaneous least squares fits to all data points displayed as described in the text with the exception of the lower lines in the bottom boxes which show the outer-sphere contribution to proton relaxivity calculated from the fitted parameters at 283.2 k (a), 298.2 k (b−d), and 302.2 K (e, f).

to another should be twice this value. Thus with $a_{GdGd} \approx 6.1$ Å and $D_{GdGd} \approx 1.2 \times 10^{-9}$ m^2 s^{-1} one can estimate $\tau_{GdGd} \approx 3 \times 10^{-10}$ s at 298 K whereas, from Figure 1, the transverse electronic relaxation time is longer than 10^{-9} s at the same

Table 2. Parameters Obtained from Analysis of the Variable-Temperature, High-Field, Multiple-Concentration Electronic Relaxation Rates[a]

complex	$(1/T)_{2e}^{0,298}$ (10^8 s^{-1})	E_0 (kJ mol^{-1})	D_{GdGd}^{298} (10^{-10} m^2 s^{-1})	E_{DGdGd} (kJ mol^{-1})	τ_{Re}^{298} (10^{-10} s)	E_{Re} (kJ mol^{-1})
$[Gd(H_2O)_8]^{3+}$	7.6 ± 0.1	8.4 ± 0.7	6.7 ± 2.3	4 ± 13		
$[Gd(DTPA)(H_2O)]^{2-}$	2.38 ± 0.02	4.9 ± 0.3	9.8 ± 0.8	4 ± 3		
[Gd(DTPA-BMA)(H_2O)]	2.67 ± 0.04	4.6 ± 0.4	7.3 ± 0.8	14 ± 5		
$[Gd(DOTA)(H_2O)]^{-}$	1.67 ± 0.02	5.1 ± 0.5	5.0 ± 0.3	7 ± 2		
[pip{Gd(DO3A)(H_2O)}$_2$]	1.67	5.1	1.8 ± 0.2	0 ± 4	1.49 ± 0.04	10 ± 1
[bisoxa{Gd(DO3A)(H_2O)}$_2$]	1.67	5.1	1.7 ± 0.1	4 ± 3	1.51 ± 0.03	5 ± 1

[a] Underlined quantities were fixed in the fitting procedure.

temperature, so that τ_d/T_{ie} will be small compared to $\omega_S\tau_d$ and the effect of the electronic relaxation rates on the spectral density functions will be minor. For the other complexes, electronicrelaxation at 5.0 T is even slower, so that the effect will be smaller and the Redfield approximation is justified.

It is difficult to estimate the distance of closest intermolecular approach for the Gd^{3+} ions in the poly(amino carboxylates). In the crystal structures of [Gd(DTPA-BMA)(H_2O)],[25] $[Eu(DOTA)(H_2O)]^-$,[26] and $[Nd(DTPA)(H_2O)]^{2-}$ [27] complexes, the metal−carbon distances within the carbon backbone are *ca.* 3.5 Å, whereas the nonbonding carboxylate oxygens are *ca.* 4.5 Å from the metal center. There will certainly be some interpenetration of these coordination spheres, so we estimate an effective radius of *ca.* 4 Å and a value of $a_{GdGd} \approx 8$ Å for all the poly(amino carboxylates).

The observed transverse electronic relaxation rates for the aqua ion and the three monomeric complexes as a function of temperature and concentration at 5.0 T were fitted using eqs 3 and 4. The distance of closest Gd−Gd approach was fixed at the values estimated above and the concentration independent contribution to the relaxation rates, denoted $1/T_{2e}^0$, was fitted to a simple exponential function (eq 5) with value $1/T_{2e}^{0,298}$ at

$$\left(\frac{1}{T_{2e}}\right)^0 = \left(\frac{1}{T_{2e}}\right)^{0,298} \exp\left\{\frac{E_0}{R}\left(\frac{1}{298.15} - \frac{1}{T}\right)\right\} \qquad (5)$$

298.15 K and activation energy E_0. The diffusion coefficient, D_{GdGd}, was similarly assumed to obey eq 6, with value D_{GdGd}^{298}

$$D_{GdGd} = D_{GdGd}^{298} \exp\left\{\frac{E_{DGdGd}}{R}\left(\frac{1}{298.15} - \frac{1}{T}\right)\right\} \qquad (6)$$

at 298.15 K and activation energy, E_{DGdGd}. The results of the fits are shown in Figures 2a to 2d and the fitted parameters for the monomers are given in Table 2. The fitted relative diffusion coefficient, D_{GdGd}^{298}, for two $[Gd(H_2O)_8]^{3+}$ complexes, is of the order of magnitude estimated above. This suggests that the theory presented here is adequate to explain the observed concentration dependence of the electronic relaxation rates. However, it must be stressed that the diffusion coefficients obtained for all the complexes are open to error due to the difficulty of estimating the distance of closest approach, a_{GdGd}.

The relaxation rates at 5.0 T for the two dimeric complexes differ from those of the other poly(amino carboxylates) in that (a) the rates are much greater, especially compared to the $[Gd(DOTA)(H_2O)]^-$ complex, which has a similar coordination structure and (b) the rates decrease rather than increase with temperature. These observations suggest that there is an additional contribution to the relaxation rates due to intramolecular dipole−dipole interactions between the two Gd^{3+} ions in the complexes. The relaxation rates for intramoleculardipole−dipole relaxation by like spins are given by eqs 7 and 8,[21] where the spectral density function, J_n^{intra}, is defined by eq 9 and r_{GdGd} is the intramolecular Gd−Gd distance. The

$$\left(\frac{1}{T_{1e}}\right)^{intra} = \frac{1}{5}\left(\frac{\mu_o}{4\pi}\right)^2 \frac{\hbar^2\gamma_S^4 S(S+1)}{r_{GdGd}^6}(2J_1^{intra} + 8J_2^{intra}) \qquad (7)$$

$$\left(\frac{1}{T_{2e}}\right)^{intra} = \frac{1}{5}\left(\frac{\mu_o}{4\pi}\right)^2 \frac{\hbar^2\gamma_S^4 S(S+1)}{r_{GdGd}^6}(3J_0^{intra} + 5J_1^{intra} + 2J_2^{intra}) \qquad (8)$$

$$J_n^{intra} = \frac{\tau_{Re}}{1 + \omega_S^2\tau_{Re}^2} \qquad (9)$$

equations are valid provided the rotation of the molecule is rapid compared to the electronic relaxation. The rotational correlation time, τ_{Re}, is assumed to have a simple exponential temperature dependence (eq 10) with value τ_{Re}^{298} at 298.15 K and activation

$$\tau_{Re} = \tau_{Re}^{298} \exp\left\{\frac{E_{Re}}{R}\left(\frac{1}{T} - \frac{1}{298.15}\right)\right\} \qquad (10)$$

energy E_{Re}. The observed transverse relaxation rates at 5.0 T and variable temperature and concentration for the two dimeric complexes were fitted using eqs 3−6 and 8−10, with a_{GdGd} fixed at 8.0 Å. The intramolecular Gd−Gd distances were estimated at $r_{GdGd} = 8.7$ Å for [pip{Gd(DO3A)(H_2O)}$_2$] and $r_{GdGd} = 9.3$ Å for [bisoxa{Gd(DO3A)(H_2O)}$_2$] on the basis of molecular mechanics calculations. The concentration independent contribution to the relaxation rates was assumed to be the sum of $(1/T_{2e})^{intra}$ and $(1/T_{2e})^0$, where $(1/T_{2e})^0$ was approximated by the values for $[Gd(DOTA)(H_2O)]^-$. The resulting fits are shown as curves in Figures 3e and 3f and the resulting parameters for the dimers are given in Table 2.

As expected, the diffusion coefficients obtained for the relatively bulky dimeric complexes are very much lower than those for the monomeric complexes, adding credence to our interpretation of the concentration-dependent part of the relaxation rates. The values obtained for the rotational correlation times, τ_{Re}^{298}, are reasonably close to those determined by ^{17}O NMR and NMRD (see below), so our model of intramolecular dipole−dipole relaxation is able to account for the magnitude of the large concentration-independent contributions to the relaxation rates observed for these two complexes. The activation energies, E_{Re}, on the other hand, are considerably lower than those obtained by ^{17}O NMR: this discrepancy almost certainly originates from uncertainty in the calculation of $1/T_{2e}^0$, approximated here by the values for $[Gd(DOTA)(H_2O)]^-$.

(25) Sanofi Nycomed, private communication.
(26) Spirlet, M.-R.; Rebizant, J.; Desreux, J. F.; Loncin, M. F. *Inorg. Chem.* **1984**, *23*, 359.
(27) Stezowski, J. J.; Hoard, J. L. *Isr. J. Chem.* **1984**, *24*, 323.

It will be useful for the analysis below to consider these dipole−dipole relaxation mechanisms in more detail. If one substitutes the fitted parameters into eqs 4 and 8 one finds that, for all complexes studied, J_0 is at least three orders of magnitude greater than either J_1 or J_2 for both inter- and intramolecular relaxation mechanisms. This has two important consequences: firstly the contribution of these mechanisms to the overall relaxation rates will be practically independent of magnetic field and secondly the contribution to the longitudinal relaxation rates will be negligibly small, since J_0 appears only in the expressions for the transverse relaxation rates (eqs 3 and 8).

Multiple-Field EPR Measurements: Relaxation due to Zero Field Splitting Interactions. The multiple magnetic field EPR measurements were analyzed using eq 1 to yield the transverse electronic relaxation rates shown in the upper boxes of Figures 3a to 3f. The data for $[Gd(H_2O)_8]^{3+}$ and [Gd(DTPA-BMA)(H_2O)] have already been published.[7,10] The other data are new. Electronic relaxation rates in Gd^{3+} complexes have generally been interpreted in terms of a zero field splitting interaction using the theory due to McLachlan,[28] where the relaxation rates are averaged over the different transitions contributing to the overall line shape. In a previous publication we showed that the transverse electronic relaxation rates in $[Gd(H_2O)_8]^{3+}$, $[Gd(PDTA)(H_2O)_2]^-$, and [Gd(DTPA-BMA)(H_2O)] could indeed be accounted for by modulation of the zero field splitting, but an average over the different relaxation *times* rather than rates gave a better description of the magnetic field dependence of the rates.[7] This approach resulted in eqs 11 and 12, where eq 11 for the longitudinal relaxation rates is that of

$$\left(\frac{1}{T_{1e}}\right)^{ZFS} = \frac{1}{25}\Delta^2\tau_v\{4S(S+1)-3\}\left(\frac{1}{1+\omega_S^2\tau_v^2}+\frac{4}{1+4\omega_S^2\tau_v^2}\right) \quad (11)$$

$$\left(\frac{1}{T_{2e}}\right)^{ZFS} = \Delta^2\tau_v\left[\frac{5.26}{1+0.372\omega_S^2\tau_v^2}+\frac{7.18}{1+1.24\omega_S\tau_v}\right] \quad (12)$$

McLachlan.[28] Δ^2 is the mean-square zero field splitting energy and τ_v is the correlation time for modulation of the zero field splitting interaction. This modulation may result either from rotation or from transient distortions of the complex. We assume that τ_v has the simple exponential temperature dependence given by eq 13 with value τ_v^{298} at 298.15 K and

$$\tau_v = \tau_v^{298}\exp\left\{\frac{E_v}{R}\left(\frac{1}{T}-\frac{1}{298.15}\right)\right\} \quad (13)$$

activation energy, E_v. It should be noted that our notation is different from that generally used in the interpretation of NMRD profiles. The zero field electronic relaxation time, τ_{s0}, that is normally quoted[3] corresponds to $(12\Delta^2\tau_v)^{-1}$ in our notation.

We found, in a previous study, that it was necessary to invoke a further, magnetic field independent electronic relaxation mechanism in order to explain the observed ^{17}O relaxation rates.[4] We proposed that there is a spin-rotation relaxation mechanism, with relaxation rates given by eq 14, where $\delta g_L^2 = \sum_i \delta g_{Li}^2$, δg_{Li}

$$\left(\frac{1}{T_{ie}}\right)^{SR} = \frac{\delta g_L^2}{9\tau_R} \qquad i = 1, 2 \quad (14)$$

being the deviations from the free electron value of the g_L values along the principal axes of the g_L tensor. τ_R is assumed to have a temperature dependence similar to that of τ_{Re}, with its own activation energy E_R (eq 15).[29,30]

$$\tau_R = \tau_R^{298}\exp\left[\frac{E_R}{R}\left(\frac{1}{T}-\frac{1}{298.15}\right)\right] \quad (15)$$

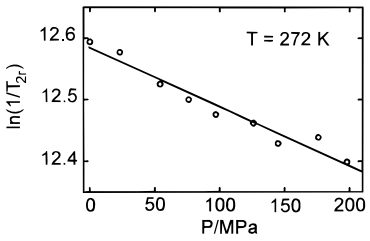

Figure 4. Pressure dependence of reduced transverse ^{17}O relaxation rates of an aqueous solution containing [bisoxa{Gd(DO3A)(H_2O)}$_2$] at 272.0 K and 9.4 T; the line represents a leasts-squares fit that yields an activation volume of $\triangle V^{\ddagger} = +(2.3 \pm 0.2)$ cm^3 mol^{-1}.

It should be noted that, although this electronic relaxation term was included in the analysis, its influence on the transverse electronic relaxation rates is negligible. Its main effect is on the longitudinal electronic relaxation rates, which influence the ^{17}O NMR data, and is used to explain a slower than expected decrease of $1/T_{1e}$ with magnetic field. The spin rotation mechanism has been described for several paramagnetic ions,[31] and it is quite reasonable that it should operate for Gd^{3+}.

The overall transverse electronic relaxation rates are thus a sum of intermolecular dipole−dipole, intramolecular dipole−dipole (dimers only), zero field splitting, and spin rotation relaxation mechanisms, with the zero field splitting contribution dominating except at high fields. Data for low concentration solutions were used in the analysis of the multiple field data, in order to minimize the contribution from intermolecular dipole−dipole relaxation. The data were fitted simultaneously with the ^{17}O NMR and NMRD data (see below) using eqs 3, 4, 6, 12, and 13 (plus eqs 8 to 10 for the dimers). There are thus 10 parameters affecting the fit to the multiple-field EPR data (Table 2) of which Δ^2, τ_v^{298} and E_v are the most important. The poor quality of the fits in Figures 3a to 3f show that, although eq 11 gives a better description of the data than the treatment by McLachlan, the relaxation theory used is only very approximate. For this reason, the variable-concentration data were not fitted simultaneously with the multiple field data, as the poor fit to the multiple field data would mask the concentration effect. The values for D_{GdGd}^{298} and E_{DGdGd} were entered as fixed parameters in the least-squares fit.

Variable-Temperature ^{17}O NMR Measurements. From the measured ^{17}O NMR relaxation rates and angular frequencies of the Gd^{3+} containing solutions, $1/T_1$, $1/T_2$, and ω, and of the acidified water reference, $1/T_{1A}$, $1/T_{2A}$, and ω_A, one can calculate the reduced relaxation rates and chemical shift, $1/T_{1r}$, $1/T_{2r}$, and

(28) McLachlan, A. D. *Proc. R. Soc. London* **1964**, *A280*, 271.

(29) One might use τ_{Re} instead of τ_R for the spin rotational mechanism, too. However, the anisotropic interaction between rotating charges and the electronic spins ("spin rotation") is dominated by correlation time for the rotation of the *g*-tensor, represented by the spin rotation tensor **C** in the Hamiltonian $\boldsymbol{H} = \boldsymbol{S}\cdot\mathbf{C}\cdot\boldsymbol{J}$, where $\boldsymbol{S}$ is the spin angular momentum operator, and $\boldsymbol{J}$ the angular rotational momentum.[30] The rotation of the *g*-tensor is linked to the rotation of the local coordination environment of Gd^{3+} and will be better described by the Gd^{3+}−water vector, measured by ^{17}O NMR and NMRD, than by the rotation of the whole complex, espcially in the case of the dimers. Therefore we choose τ_R rather than τ_{Re} as correlation time for the spin rotational relaxation mechanism.

(30) Banci, L.; Bertini, I.; Luchinat, C. *Nuclear and Electron Relaxation*; VCH: Weinheim, 1991; pp 83−85.

(31) Atkins, P. W.; Kivelson, D. *J. Chem. Phys.* **1966**, *44*, 169.

$\Delta\omega_r$, which may be written as in eqs 16−18,[32,33] where $1/T_{1m}$,

$$\frac{1}{T_{1r}} = \frac{1}{P_m}\left[\frac{1}{T_1} - \frac{1}{T_{1A}}\right] = \frac{1}{T_{1m} + \tau_m} + \frac{1}{T_{1os}} \tag{16}$$

$$\frac{1}{T_{2r}} = \frac{1}{P_m}\left[\frac{1}{T_2} - \frac{1}{T_{2A}}\right] = \frac{1}{\tau_m}\frac{T_{2m}^{-2} + \tau_m^{-1}T_{2m}^{-1} + \Delta\omega_m^2}{(\tau_m^{-1} + T_{2m}^{-1})^2 + \Delta\omega_m^2} + \frac{1}{T_{2os}} \tag{17}$$

$$\Delta\omega_r = \frac{1}{P_m}(\omega - \omega_A) = \frac{\Delta\omega_m}{(1 + \tau_m T_{2m}^{-1})^2 + \tau_m^2\Delta\omega_m^2} + \Delta\omega_{os} \tag{18}$$

$1/T_{2m}$ are the relaxation rates in the bound water, $\Delta\omega_m$ is the chemical shift difference between bound water and bulk water (in the absence of a paramagnetic interaction with the bulk water), P_m is the mole fraction of bound water, and τ_m is the mean residence time (or inverse exchange rate, $1/\tau_m = k_{ex}$) of water molecules in the inner-coordination sphere. The total outer-sphere contributions to the reduced relaxation rates and chemical shift are represented by $1/T_{1os}$, $1/T_{2os}$, and $\Delta\omega_{os}$. The temperature and magnetic field dependence of the reduced relaxation rates and chemical shifts for the six complexes studied are shown in Figures 3a to 3f. The data for the aqua ion and the three commercial contrast agents have been at least partially published.[4,9,10] The 1.4-T data for $[Gd(DTPA)(H_2O)]^{2-}$ and $[Gd(DOTA)(H_2O)]^-$ and all the data for the two dimeric complexes are presented here for the first time.

We have shown in previous publications that the outer-sphere contributions in eqs 16 and 17 are negligible.[9] We used the full eqs 16 and 17, with the outer-sphere terms set to zero, in the analysis. However, it is useful to consider the simplified eqs 19 and 20, where the contribution of $\Delta\omega_m$ in eq 17 is

$$\frac{1}{T_{1r}} = \frac{1}{T_{1m} + \tau_m} \tag{19}$$

$$\frac{1}{T_{2r}} = \frac{1}{T_{2m} + \tau_m} \tag{20}$$

assumed to be negligible. Since τ_m decreases, while T_{1m} and T_{2m} generally increase, with increasing temperature the sign of the temperature dependence of $1//T_{1r}$ or $1/T_{2r}$ will depend on which term dominates in the denominator of eqs 17 and 18. The maxima observed in the temperature dependence of $1/T_{2r}$ (Figures 3b to 3f) are characteristic of the changeover from the "fast exchange" regime at high temperatures, where T_{2m} is the dominant term in eq 18, to the "slow exchange" regime at low temperatures, where τ_m is the dominant term. The changeover between fast and slow exchange limits is also manifested in $\Delta\omega_r$, the maxima in $1/T_{2r}$ corresponding to the points of inflection in $\Delta\omega_r$. At high temperatures, the inner-sphere contribution to $\Delta\omega_r$ is given by the chemical shift of the bound water molecules, which is determined by the hyperfine interaction between the Gd^{3+} electron spin and the ^{17}O nucleus *via* eq 21,[34] where g_L is the isotropic Landé g factor ($g_L = 2.0$ for

$$\Delta\omega_m = \frac{g_L\mu_B S(S+1)B}{3k_B T}\frac{A}{\hbar} \tag{21}$$

Gd^{3+}), S is the electron spin ($S = {}^7/_2$ for Gd^{3+}), $A/\hbar$ is the hyperfine or scalar coupling constant, and B is the magnetic field. We assume that the outer-sphere contribution to $\Delta\omega_r$ has a similar temperature dependence to $\Delta\omega_m$ and is given by eq 22 where C_{os} is an empirical constant.[4,9]

$$\Delta\omega_{os} = C_{os}\Delta\omega_m \tag{22}$$

The ^{17}O longitudinal relaxation rates in Gd^{3+} solutions are dominated by the dipole−dipole and quadrupolar mechanisms, and are given by eq 23,[9,21,35] where γ_I is the nuclear gyromagnetic ratio ($\gamma_I = -3.626 \times 10^7$ rad s^{-1} T^{-1} for ^{17}O), r_{GdO} is the mean Gd^{3+}−O distance, I is the nuclear spin ($I = {}^5/_2$ for ^{17}O), χ is the quadrupolar coupling constant, η an asymmetry parameter, and $\tau_{di} = \tau_m^{-1} + T_{ie}^{-1} + \tau_R^{-1}$. Using the quadrupolar coupling constant for acidified water, $\chi(1 + \eta^2/3)^{1/2} = 7.58$ MHz,[36] and estimating $r = 2.5$ Å from the available crystal structures,[25−27] the dipole−dipole mechanism (the first term in eq 22) is expected to contribute *ca.* 70% of $1/T_{1m}$. τ_R is the rotational correlation time for the Gd^{3+}−O vector. While, for the monomeric complexes, this is equivalent to the rotational correlation time of the whole complex, this is not necessarily true for the dimers, as part of the molecule may rotate independently of the rest. We therefore differentiate τ_R for the Gd^{3+}−O vector from τ_{Re}, which influences the electronic relaxation rates.

$$\frac{1}{T_{1m}} = \left[\frac{1}{15}\left(\frac{\mu_0}{4\pi}\right)^2\frac{\hbar^2\gamma_I^2\gamma_S^2}{r_{GdO}^6}S(S+1)\right]\left[6\tau_{d1} + 14\frac{\tau_{d2}}{1 + \omega_S^2\tau_{d2}}\right] + \frac{3\pi^2}{10}\frac{2I+3}{I^2(2I-1)}\chi^2(1 + \eta^2/3)\tau_R \tag{23}$$

The ^{17}O transverse relaxation rates in bound water in Gd^{3+} solutions are dominated by the scalar relaxation mechanism, and are given to an excellent approximation by eq 24,[9] where

$$\frac{1}{T_{2sc}} = \frac{(A/\hbar)^2}{3}S(S+1)\left[\tau_{1S} + \frac{\tau_{2S}}{1 + \omega_S^2\tau_{2S}^2}\right] \tag{24}$$

$1/\tau_{iS} = 1/\tau_m + 1/T_{ie}$. It is the efficiency of this relaxation mechanism that allows the determination of faster exchange rates with ^{17}O NMR, as it shortens T_{2m} in eq 20, so that the slow exchange regime can be observed. The mechanism is not effective in longitudinal relaxation due to the absence of the τ_{1s} term in eq 24, and so has been neglected in eq 23 above. Scalar relaxation is much less important in proton relaxation, because the protons are more distant from the paramagnetic center so that the scalar coupling constant for the electron−proton interaction is small. In NMRD, where longitudinal proton relaxivity is measured, the scalar relaxation contribution is negligible.[3] While this simplifies the treatment of NMRD data, it means that the method is a poor measure of water exchange compared to ^{17}O NMR.

The electronic relaxation rates are given by the equations derived in the previous two sections. Since the τ_{1s} term dominates in eq 24 it is the longitudinal electronic relaxation rates that contribute to the ^{17}O transverse relaxation rates. As discussed above, the dipole−dipole electronic relaxation mechanisms are ineffective in longitudinal electronic relaxation, so that it is the zero field splitting and spin rotation contributions that dominate (parameters Δ^2, τ_v^{298}, E_v, δ_L^2, τ_{Re}^{298}, and E_{Re}).

The longitudinal ^{17}O NMR relaxation rates are essentially in the fast exchange regime (little influence of τ_m) and are thus

(32) Swift, T. J.; Connick, R. E. *J. Chem. Phys.* **1962**, 37, 307.
(33) Zimmermann, J. R.; Brittin, W. E. *J. Phys. Chem.* **1957**, *61*, 1328.
(34) Brittain, H. G.; Desreux, J. F. *Inorg. Chem.* **1984**, *23*, 4459.
(35) Kowalewski, J.; Nordenskjöld, L.; Benetis, N.; Westlund, P.-O. *Prog. Nucl. Magn. Reson. Spectrosc.* **1985**, *17*, 141.
(36) Halle, B.; Wennerström, H. *J. Chem. Phys.* **1981**, *75*, 1928.

influenced by four parameters: τ_R^{298}, E_R, r_{GdO}, and the quadrupolar coupling constant $\chi(1 + \eta^2/3)^{1/2}$.

The binding time (or exchange rate, k_{ex}) of water molecules in the inner sphere is assumed to obey the Eyring equation (eq 25) where $\Delta S^{\ddagger}$ and $\Delta H^{\ddagger}$ are the entropy and enthalpy of

$$\frac{1}{\tau_m} = k_{ex} = \frac{k_B T}{h}\exp\left\{\frac{\Delta S^{\ddagger}}{R} - \frac{\Delta H^{\ddagger}}{RT}\right\} = \frac{k_{ex}^{298} T}{298.15}\exp\left\{\frac{\Delta H^{\ddagger}}{R}\left(\frac{1}{298.15} - \frac{1}{T}\right)\right\} \quad (25)$$

activation for the exchange process and k_{ex}^{298} is the exchange rate at 298.15 K.

The data were fitted simultaneously with the EPR and NMRD data using eqs 2−4, 6−18, and 21−25. There are thus 6, 13, and 14 parameters that affect the fits of the $1/T_{1r}$, $1/T_{2r}$, and $\Delta\omega_r$ data, respectively (Table 3).

NMRD. The measured increases of longitudinal proton relaxation rates, compared to a pure water or serum reference, normalized to millimolar Gd^{3+} concentration, are shown as the bottom boxes in Figures 3a to 3f (the data for $[Gd(H_2O)_8]^{3+}$ and $[Gd(DOTA)(H_2O)]^-$ are literature data,[3,37] the other data were provided by Sanofi Nycomed[38]). These NMRD profiles contain contributions from both inner-sphere and outer-sphere relaxivity, as described in the introduction (eq 26). Since the

$$R_1 = R_{1is} + R_{1os} \quad (26)$$

normalization of the relaxivity is different from that used for $1/T_{1r}$ in ^{17}O NMR, we adopt the usual notation R_1 for the longitudinal proton relaxivity. However, it should be borne in mind that these two quantities are analogous. The inner-sphere contribution to overall proton relaxivity in s^{-1} mol^{-1} L can be described by eq 27 (analogous to eq 18), where c is the

$$R_{1is} = \frac{c}{1000}\frac{q}{55.5}\frac{1}{T_{1m}^H + \tau_m} \quad (27)$$

gadolinium concentration in mol L^{-1} and q the number of inner-sphere water molecules. The longitudinal relaxation rate of inner-sphere water protons, $1/T_{1m}^H$, is given by eq 28,[39,40] where

$$\frac{1}{T_{1m}} = \frac{2}{15}\frac{\hbar^2\gamma_S^2\gamma_I^2}{r_{GdH}^6} S(S+1)\left[\frac{3\tau_{d1}}{1+\omega_I^2\tau_{d1}^2} + \frac{7\tau_{d2}}{1+\omega_S^2\tau_{d2}^2}\right] \quad (28)$$

γ_S (γ_I) is the electron (proton) gyromagnetic ratio ($\gamma_I = 2.765 \times 10^8$ rad s^{-1} T^{-1} for protons), r_{GdH} is the effective distance between the gadolinium electron spin and the water protons, ω_I is the proton resonance frequency at the magnetic field applied, and τ_{di} is given by eq 29, where τ_R is now the

$$\frac{1}{\tau_{di}} = \frac{1}{\tau_m} + \frac{1}{\tau_R} + \frac{1}{T_{ie}} \qquad i = 1, 2 \quad (29)$$

correlation time for the rotation of the Gd^{3+}−proton vector. We assume that, for both proton and ^{17}O NMR as well as for the spin rotational mechanism (eqs 14 and 15), τ_R is given by the overall rotational correlation time of the gadolinium-water vector.[29] As described above, the scalar contribution to longitudinal proton relaxation is negligible and has been ignored in eq 28.

The outer-sphere contribution to proton relaxivity can be described by eq 30,[3,20] where N_A is the Avogadro constant, and

$$R_{1os} = \frac{6400 N_A \pi}{81}\left(\frac{\mu_0}{4\pi}\right)^2 \frac{\hbar^2\gamma_S^2\gamma_1^2}{a_{GdH} D_{GdH}} S(S+1)[3J_{os}(\omega_1, T_{1e}) + 7J_{os}(\omega_S, T_{2e})] \quad (30)$$

the spectral density function, J_{os}, is given by eq 31. D_{GdH} is

$$J_{os}(\omega, T_{ie}) = \mathrm{Re}\left[\left\{1 + \frac{1}{4}\left(i\omega\tau_{GdH} + \frac{\tau_{GdH}}{T_{ie}}\right)^{1/2}\right\}\Big/ \left\{1 + \left(i\omega\tau_{GdH} + \frac{\tau_{GdH}}{T_{je}}\right)^{1/2} + \frac{4}{9}\left(i\omega\tau_{GdH} + \frac{\tau_{GdH}}{T_{je}}\right) + \frac{1}{9}\left(i\omega\tau_{GdH} + \frac{\tau_{GdH}}{T_{je}}\right)^{3/2}\right\}\right] \quad \text{with } j = 1, 2 \quad (31)$$

the diffusion coefficient for diffusion of a water proton away from a Gd^{3+}complex (approximately the sum of the diffusion coefficient of water and that of the complex), and a_{GdH} is the distance of closest approach of a second sphere water proton to the Gd^{3+} center. The correlation time, $\tau_{GdH} = a_{GdH}^2/D_{GdH}$, corresponds to the time taken for a water proton to diffuse away from the vicinity of a Gd^{3+} complex.

To our knowledge, no published variable-temperature NMRD study has made use of an explicit temperature dependence of the diffusion coefficient, which has been fitted independently for each temperature available. We introduce an additional constraint on the data by assuming an exponential law (eq 32)

$$D_{GdH} = D_{GdH}^{298}\exp\left\{\frac{E_{DGdH}}{R}\left(\frac{1}{298.15} - \frac{1}{T}\right)\right\} \quad (32)$$

for the diffusion coefficient, where D_{GdH}^{298} is the value at 298.15 K and E_{DGdH} is the activation energy for the process.

The data were fitted, simultaneously with the EPR and ^{17}O NMR data, using eqs 26−32, together with eqs 2−4 and 6−18 describing the electronic relaxation rates that enter in eq 28. There are thus 18 parameters that influence the fits to the NMRD profiles (Table 3).

Simultaneous Fitting of EPR, NMRD, and ^{17}O NMR Data. The parameters that influence the fits to the different types of measurement, according to the theoretical treatment presented above, are summarized in Table 3. It can be seen that there are a total of 21 parameters! The parameters that influence the small concentration-dependent contribution to the EPR relaxation rates, a_{GdGd}, D_{GdGd}^{298}, and E_{DGdGd}, were fixed at the values obtained in the independent analysis given in the first section of the results. Following previous NMRD and structural studies, the distance of closest approach of a water proton to a Gd^{3+} center, a_{GdH}, was fixed at 3.5 Å, and the inner-sphere Gd^{3+}−H distance, r_{GdH}, was fixed at 3.1 Å. In addition, either the quadrupolar coupling constant, $\chi(1 + \eta^2/3)^{1/2}$, was fixed at its value for acidified water, 7.58 MHz, or the inner-sphere Gd^{3+}−O distance, r_{GdO}, was fixed on the basis of structural studies at 2.5 Å (attempts to fix both these parameters led to poor fits to the data). For the dimers, r_{GdGd} was fixed at the values given in the separate section above, and τ_{Re}^{298} and E_{Re} were allowed to vary. This left 15 adjustable parameters in the least-squares fits of the data for the monomers and 17 for the dimers.

(37) Aime, S.; Benetello, F.; Bombieri, G.; Botta, M. Submitted for publication.
(38) Kellar, K.; Brown, R. D., III. Private communication.
(39) Bloembergen, N. *J. Chem. Phys.* **1957**, *27*, 572.
(40) Solomon, I. *Phys. Rev.* **1955**, *99*, 559.

Table 3. The Parameters That Influence the Fits of the Different Types of Measurements[a]

parameter	EPR ($1/T_{2e}$)	^{17}O NMR ($1/T_{1r}$)	^{17}O NMR ($1/T_{2r}$)	^{17}O NMR ($\Delta\omega_r$)	NMRD (R_1)
τ_m (k_{ex})		X	X	X	X
$\Delta H^{\ddagger}$		X	X	X	X
$A/\hbar$			X	X	
C_{os}				X	
τ_R^{298}		X			X
E_R		X			X
τ_v^{298}	X	x	X	X	X
E_v	X	x	X	X	X
Δ^2	X	x	X	X	X
δg_L^2	x	x	X	X	X
a_{GdH}					X
D_{GdH}^{298}					X
E_{DGdH}					X
a_{GdGd}	X		x	x	x
D_{GdGd}^{298}	X		x	x	x
E_{DGdGd}	X		x	x	x
τ_{Re}^{298}	X (dimers)		X	X	X
E_{Re}	X (dimers)		X	X	X
$\chi^2(1 + \eta^2/3)$		X			
r_{GdO}		X			
r_{GdH}					X
r_{GdGd}	X (dimers)	X (dimers)	X (dimers)	X (dimers)	X (dimers)

[a] A capital X indicates that a parameter has an influence, and a small x indicates a minor influence.

The data were fitted simultaneously using the equations specified in the separate sections above, with either $\chi(1 + \eta^2/3)^{1/2} = 7.58$ MHz and r_{GdO} adjustable or $\chi(1 + \eta^2/3)^{1/2}$ adjustable and $r_{GdO} = 2.5$ Å. For the macrocyclic complexes, E_v had to be fixed at a small positive value, otherwise negative activation energies would result (typically: (-1 ± 2) kJ mol^{-1}). The weighting of the data sets was adjusted to give the best subjective compromise in the quality of fits to the different data sets: the optimum weighting factors were found to be 10 for the 9.4- and 4.7-T ^{17}O NMR data, six for the 1.4-T ^{17}O NMR relaxation rates, and unity for the other data sets. The lower weighting of the electronic relaxation rates is justified by the relatively poor agreement of experiment and theory, and that of the NMRD data by the relatively large number of data points and the fact that the data enter linearly rather than logarithmically into the fit. The results of the least-squares fits are shown as the curves in Figure 4. For the monomeric complexes the quality of the fits is somewhat reduced compared to those obtained from fits of the individual techniques,[4,9,10] showing that the effect of the greater constraint on the data more than compensates the increase in the number of adjustable parameters. The parameters obtained from the least-squares fits are given in Table 4. In the two fits with either $\chi(1 + \eta^2/3)^{1/2}$ or r_{GdO} fixed, the values obtained for the remaining parameters were identical.

Variable-Pressure NMR Measurements. The pressure dependence of the reduced transverse relaxation rates, $1/T_{2r}$, for [bisoxa{Gd(DO3A)(H_2O)}$_2$] at 272.0 K and 9.4 T is shown in Figure 4. At this temperature and magnetic field, $1/T_{2r}$ is near the slow exchange limit and so is dominated by τ_m (using the parameters in Table 4, T_{2m} is only *ca.* 4% of the denominator in eq 19). The decrease of $1/T_{2r}$ with pressure in Figure 4 is, therefore, due to a slowing of the water exchange process. The pressure dependence of the water exchange rate may be written as in eq 33, where it is assumed that the activation volume,

$$\frac{1}{\tau_m} = k_{ex} = (k_{ex})_0^T \exp\left\{-\frac{\Delta V^{\ddagger}}{RT}P\right\} \qquad (33)$$

$\Delta V^{\ddagger}$, is independent of pressure, and $(k_{ex})_0^T$ is the exchange rate at zero pressure and temperature T.[4,9−11]

We performed a least-squares fit of the data in Figure 4 using eqs 11−14, 17, 21, 24, and 33 with $(k_{ex})_0^T$ and $\Delta V^{\ddagger}$ as fitted parameters. The scalar coupling constant was found previously to be independent of pressure,[41] so we assume that it is constant and equal to the value in Table 4. The mean-square deviation of the g_L-tensor, Δg_L^2, was also assumed independent of pressure. We calculated the correlation times, τ_v and τ_R at zero pressure and 272.0 K, using eqs 10 and 13 and the parameters in Table 4. Ascribing a pressure dependence equivalent to an activation volume of ± 5 cm^3 mol^{-1} to these correlation times had a negligible effect on the fitted parameters (as expected, since the contribution of T_{2m} in eq 16 is so small). The fitted function is shown in Figure 4. The fit parameters are $(k_{ex})_0^{272} = (3.1 \pm 0.3) \times 10^5$ s^{-1} and $\Delta V^{\ddagger} = +2.3 \pm 0.2$ cm^3 mol^{-1}.

Discussion

Simultaneous Treatment of EPR, ^{17}O NMR, and NMRD Data. As illustrated by Table 3, there are a large number of parameters influencing the data obtained by the different techniques. This is particularly the case for NMRD: even if we remove the additional parameters originating from our more complete treatment of the electronic relaxation, there are still seven parameters required to fit a single NMRD profile. It has been possible in the past to separate these parameters to some extent, since different parameters affect the profile at different magnetic fields (proton frequencies). Thus, electronic relaxation usually dominates the dipole−dipole correlation time for inner-sphere relaxivity at low field, and produces the first dispersion at around 3−4 MHz, whereas rotation dominates at higher fields and determines the shape of the dispersion at around 30 MHz. The combination of the shapes of the curves with the magnitude at low field can allow r_{GdH} to be fixed reasonably well. However, there remains a considerable uncertainty due to the fact that outer-sphere relaxivity makes up around 50% of the overall profile.

^{17}O NMR has the advantage that the outer-sphere contributions to the relaxation rates are negligibly small: this is a consequence of the oxygen nucleus being closer to the paramagnetic center when bound in the inner-sphere. In addition, the longitudinal relaxation rates are dominated by the dipole−dipole and quadrupolar relaxation rates, for which at the fields employed rotation determines the correlation time, while the transverse relaxation rates are dominated by scalar relaxation, which is insensitive to rotation of the complex. This scalar relaxation mechanism is highly efficient and often results in a kinetically controlled "slow-exchange" region at low temperatures. These facts have allowed a better separation of certain parameters, especially those describing the water exchange process. The EPR results are in principle simpler to interpret, since they are only affected by the transverse relaxation rates. However, we have seen that the electronic relaxation rates are themselves complicated, being determined by a large number of parameters and not very well described by the theories used.

Since the data from all three techniques are influenced by a number of common parameters, it is clear that there will be an increase in the constraints placed on these parameters by a simultaneous least-squares fit. This is evident in the reduced quality of the fits in Figures 3a to 3f compared to separate fits.[4,9,10] As well as fitting the data sets simultaneously we have increased the constraint on the NMRD data at different temperatures compared to previous studies. We have assumed

(41) Cossy, C.; Helm, L.; Merbach, A. E. *Inorg. Chem.* **1989**, *28*, 2699.

Table 4. Parameters Obtained from the Simultaneous Fitting of EPR, ^{17}O NMR, and NMRD Data

ligand/parameter	aqua	DTPA	DTPA-BMA	DOTA	pip(DO3A)$_2$	bisoxa(DO3A)$_2$
$k_{ex}^{298}/10^6\ s^{-1}$	804 ± 60 (830 ± 95)	3.3 ± 0.2 (4.1±0.3)	0.45 ± 0.01 (0.43 ± 0.02)	4.1 ± 0.2 (4.8 ± 0.4)	1.5 ± 0.1	1.4 ± 0.1
$\Delta H^{\ddagger}$/kJ mol^{-1}	15.3 ± 1.3 (14.9 ± 1.3)	51.6 ± 1.4 (52.0±1.4)	47.6 ± 1.1 (46.6 ± 1.3)	49.8 ± 1.5 (48.8 ± 1.6)	34.2 ± 1.8	38.5 ± 1.8
$\Delta S^{\ddagger}$/J mol^{-1} K^{-1}	−23.1 ± 4.0 (−24.1 ± 4.1)	+53.0 ± 4.7 (56.2±5.0)	+22.9 ± 3.6 (+18.9 ± 4.0)	+48.5 ± 4.9 (46.6 ± 6.0)	−11.7 ± 6.3	1.7 ± 6.3
$\Delta V^{\ddagger}$/cm^3 mol^{-1}	(−3.3 ± 0.2)	+(12.5 ± 0.2)	(+7.3 ± 0.2)	(+10.5 ± 0.2)		+2.3 ± 0.2
$A/\hbar$ /10^{6}rad s^{-1}	−5.3 ± 0.1 (−5.3 ± 0.2)	−3.8 ± 0.2 (−3.6 ± 0.3)	−3.8 ± 0.2 (−3.6 ± 0.3)	−3.7 ± 0.2 (−3.8 ± 0.2)	−3.8 ± 0.1	−4.2 ± 0.1
C_{os}	0.0 (0.0)	0.18 ± 0.04 (0.13 ± 0.06)	0.11 ± 0.04 (0.13 ± 0.06)	0.21 ± 0.04 (0.13 ± 0.06)	0.2[b]	0.2[b]
τ_R^{298}/ps	41 ± 2 (29 ± 2)	58 ± 11 (103 ± 10)	66 ± 11 (167 ± 5)	77 ± 4 (90 ± 15)	171 ± 12	106 ± 14
E_R/kJ mol^{-1}	15.0 ± 1.3 (15.1 ± 1.5)	17.3 ± 0.8 (18 ± 2)	21.9 ± 0.5 (21.6 ± 0.1)	16.1 ± 7.4 (17 ± 3)	20.4 ± 0.6	21.7 ± 0.6
τ_v^{298}/ps	7.3 ± 0.5 (7.2 ± 0.7)	25 ± 1 (0.25 ± 0.01)	25 ± 1 (34 ± 8)	11 ± 1 (0.11 ± 0.01)	19 ± 2	15 ± 1
E_v/kJ mol^{-1}	18.4 ± 1.4 (15.4 ± 1.1)	1.6 ± 1.8 (1.6 ± 1.8)	3.9 ± 1.4 (9 ± 2)	1.0 (6 ± 4)	1.0	1.0
$\Delta^2/10^{20}\ s^{-2}$	1.19 ± 0.09 (0.93 ± 0.04)	0.46 ± 0.02 (0.15)	0.41 ± 0.02 (0.38 ± 0.02)	0.16 ± 0.01 (0.12)	0.17 ± 0.01	0.21 ± 0.02
$\delta g_L^2/10^{-2}$	0.0	1.2 ± 0.3	0.8 ± 0.2 (1.7 ± 0.4)	1.9 ± 0.3	4.0 ± 0.5	2.8 ± 0.4
$D_{GdH}^{298}/10^{-10}\ m^2\ s^{-1}$	23	20 ± 3	23 ± 2	22 ± 1	29 ± 3	20 ± 3
E_{DGdH}/kJ mol^{-1}	22.0	19.4 ± 1.8	12.9 ± 2.1	20.2 ± 1.1	22.0	22.0
τ_{Re}^{298}/ps					185 ± 31	163 ± 39
E_{Re}/kJ mol^{-1}					8.2 ± 5.1	4.8 ± 7.4
$\chi(1+\eta^2/3)^{1/2}$/MHz	7.58/2.0 ± 2.3	7.58/14 ± 2	7.58/18 ± 2	7.58/10 ± 1	7.58/13 ± 1	7.58/16 ± 2
r_{GdO}/Å	2.76 ± 0.06/2.5	2.20 ± 0.09/2.5	2.12 ± 0.04/2.5	2.38 ± 0.03/2.5	2.25 ± 0.04/2.5	2.13 ± 0.06/2.5

[a] The values in brackets are those obtained in our previous publications. For previous publications see refs 10 {$[Gd(H_2O)^{sa}]^{3+}$}, 9 {$[Gd(DTPA)(H_2O)]^{2-}$ and $[Gd(DOTA)(H_2O)]^-$}, and 4 {[Gd(DTPA-BMA)(H_2O)]}. Underscored parameters were fixed in the least-squares procedure. [b] C_{os} was fixed to the reasonable value of 0.2. If C_{os} is adjusted, the fit yields values of 0.35 and 0.38 for pip(DO3A)$_2$ and bisoxa(DO3A)$_2$, respectively, which is excessively high by comparison with the values obtained for other Gd^{3+} complexes. Furthermore, no experimental evidence for such high values was perceivable from the chemical shift data. With C_{os} adjusted, the values obtained for $\delta g_L^2/10^{-2}$ are 2.7 ± 0.5 and 1.9 ± 0.4, for $A/\hbar/10^6$ rad s^{-1} −3.3 ± 0.2 and −3.5 ± 0.2, respectively. The other values do not change significantly.

physically reasonable exponential or Eyring behavior for the different correlation times (eqs 6, 10, 13, 15, and 25), rather than fitting independent values at the three temperatures. In addition, in eqs 11 and 12, we have implicitly assumed that the mean-square zero-field splitting energy, Δ^2, is independent of temperature: the values of τ_{S0} and τ_v fitted to NMRD profiles at different temperatures often lead to Δ^2 values that vary in a random, physically unreasonable manner with temperature.

The results obtained for the monomers are compared in Table 4 with those obtained from previous ^{17}O NMR and EPR studies. The parameters describing water exchange, k_{ex}^{298}, $\Delta H^{\ddagger}$, and $\Delta S^{\ddagger}$, are similar to those obtained from previous studies, confirming that ^{17}O NMR is an accurate probe of water-exchange kinetics. The scalar coupling constant, $A/\hbar$, is essentially determined by the ^{17}O chemical shifts, and so is little changed in the different analyses. The electronic relaxation parameters, τ_v^{298}, E_v and Δ^2, are similar to those found in previous studies for $[Gd(H_2O)_8]^{3+}$ and [Gd(DTPA-BMA)(H_2O)] showing that the definition of the electronic parameters by ^{17}O NMR and EPR methods is consistent with the NMRD profiles. The discrepancies seen in these parameters compared to our previous study of $[Gd(DOTA)(H_2O)]^-$ and $[Gd(DTPA)(H_2O)]^{2-}$ arise from the fact that this previous study was based entirely on ^{17}O NMR data at only two magnetic fields, and not from an inconsistency between ^{17}O NMR, EPR, and NMRD data. This illustrates the importance of making measurements over a large range of magnetic fields, and of using data from more than one technique.

The rotational correlation time, τ_R^{298}, is consistently shorter than the values obtained in our previous studies, while its activation energy E_R is virtually unchanged. There is a discrepancy between the rotational correlation time determined by the shape of the NMRD profiles and that determined by the magnitude of the ^{17}O longitudinal relaxation rates. We have allowed for this by letting either the overall quadrupolar coupling constant, $\chi(1+\eta^2/3)^{1/2}$, or the Gd^{3+}−O distance, r_{GdO}, vary. This has the effect of changing the magnitude of either the quadrupolar or the dipole−dipole relaxation contribution to $1/T_{1r}$ (eq 23) for a given value of τ_R. It is known that the quadrupolar coupling constant in water will be changed when an ^{17}O nucleus approaches an ionic charge. It is reported in a recent study of keto ligands, such as $(acac)^-$, complexed to different paramagnetic metals, that the ^{17}O quadrupolar coupling constant, χ, varies between 7.6 and 15.4 MHz,[42] so that our fitted values are perhaps not unreasonable compared to the pure water value of $\chi(1+\eta^2/3)^{1/2} = 7.58$ MHz that we have used in previous studies. With the quadrupolar coupling constant fixed, the r_{GdO} distances obtained are about 10% shorter than those expected from various structural studies. Although deviations from the point-dipole approximation make the effective electron-spin nucleus distance shorter than the ion−nucleus distance,[35] one would not expect a deviation as large as 10% for an ion such as Gd^{3+}, with little tendency for charge transfer to ligands. In reality, both $\chi(1+\eta^2/3)^{1/2}$ and r_{GdO} probably deviate to some extent from their expected values so that, while ^{17}O longitudinal relaxation rates may be useful for comparative studies of rotational correlation times in a series of similar complexes, the absolute values obtained should be treated with some caution. NMRD is probably a better measure of absolute values since the rotation correlation time contributes to the shape, as well as the overall magnitude, of the NMRD profiles (in addition r_{GdH} should deviate less than r_{GdO} from the point-dipole approximation). On the other hand, variable-temperature measurements are, with current technology, more convenient for

(42) Champmartin, D.; Rubini, P. *Inorg. Chem.* **1996**, *35*, 179.

^{17}O NMR than for NMRD, so that the combined approach is very useful for determining the activation energy for rotation.

Of the other fitted parameters, C_{os} is similar to the values obtained in our previous studies of $[Gd(H_2O)_8]^{3+}$ and [Gd(DTPA-BMA)(H_2O)].[4,10] The larger discrepancies for $[Gd(DTPA)(H_2O)]^{2-}$ and $[Gd(DOTA)(H_2O)]^{-}$ are influenced by the different electronic relaxation parameters. The values obtained for δg_L^2 are significantly different from those obtained in our previous studies. This is certainly due to the change in τ_R in comparison to previous ^{17}O NMR studies (*vide supra*).

Comparison with previous studies leads us to believe that the parameters obtained from our simultaneous least-squares fits represent a more self-consistent parameter set than those obtained from individual techniques. The simultaneous fits are a critical test of the relaxation theories used in the data analysis. The quality of the fits obtained suggests that, with the exception of the EPR treatment, the theories used are satisfactory. We are therefore confident in the new values that we have obtained for the two dimeric complexes.

Structural Parameters. The only parameters relevant to the structure of the complexes that are obtained from our fits are r_{GdO} and $A/\hbar$. The former is heavily influenced by the interplay with the quadrupolar coupling constant as discussed above, and we do not attach any significance to the variation of this value from one complex to another. The scalar coupling constant, $A/\hbar$, determined from the ^{17}O NMR shifts, is a measure of the Gd^{3+} spin density at the ^{17}O nucleus. The value should be approximately the same for all the complexes, since r_{GdO} does not vary significantly. The values for the different contrast agents are indeed very similar. This is evidence that our assumption of one inner-sphere water molecule is correct, since the number of water molecules enters directly in our calculation of $\Delta\omega_r$. This is in agreement with specific structural studies of the two dimeric complexes using X-ray diffraction, molecular mechanics calculations, and UV−visible spectroscopy.[43]

Electronic Relaxation. The theory governing electronic relaxation rates and their effect on NMR relaxation rates is undoubtedly the least well understood part of our data analysis. Electronic relaxation in Gd^{3+} complexes has generally been explained in terms of a zero-field splitting interaction. Our previous ^{17}O NMR measurements have led us to propose that there is an additional spin-rotational contribution to the electronic relaxation rates.[4] Our high-field EPR measurements have demonstrated two further electronic relaxation mechanisms, which have not previously been reported for Gd^{3+} complexes. The concentration dependence of the electronic relaxation rates at a field of 5.0 T suggested an intermolecular dipole−dipole relaxation mechanism. This was analyzed in terms of an estimated distance of closest approach of two complexes, a_{GdGd}, and a relative diffusion coefficient for one complex with respect to another, D_{GdGd}, with associated activation energy E_{DGdGd}. The values obtained for D_{GdGd}^{298} are quite reasonable, and as expected are lower than the relative diffusion coefficient of water protons with respect to a complex, D_{GdH}^{298}. In addition, the values for the bulky dimeric complexes are significantly lower than those for the monomeric complexes. Although we hesitate to give too much weight to the absolute values obtained, these facts suggest that we are indeed observing a diffusion-related phenomenon, and that the applied theory is at least approximately correct.

The relatively large electronic relaxation rates of the two dimeric complexes at 5.0 T, compared to those for the macrocyclic monomer $[Gd(DOTA)(H_2O)]^{-}$, suggested strongly that, in addition to the intermolecular interaction, an intramolecular interaction between the two Gd^{3+} ions in each dimeric complex could produce a relaxation effect. The data were analyzed in terms of the intramolecular $Gd^{3+}-Gd^{3+}$ distance, estimated from structural studies, and a rotational correlation time of the $Gd^{3+}-Gd^{3+}$ vector, τ_{Re}, with associated activation energy, E_{Re}. The rotational correlation times obtained, from both the independent fit (Table 2) and the simultaneous fit (Table 4), were quite reasonable, although the activation energies obtained were rather low. This suggests that the applied theory is basically correct, but that the activation energies are determined incorrectly due to the difficulties associated with separating the zero-field splitting and intramolecular dipole−dipole contributions to the relaxation rates.

The parameters describing the zero-field splitting interaction, τ_v^{298}, E_v, and Δ^2, are determined by the EPR data, but also by the ^{17}O NMR and NMRD data. This is potentially problematic in the simultaneous fits, as the theory for the influence of electronic relaxation rates on nuclear relaxation assumes essentially that the EPR line shape is perfectly Lorentzian. As pointed out by one of the pioneers of NMRD,[3] NMR relaxation in the presence of a paramagnetic center can be likened to an extreme off-resonance EPR experiment.[44] The nucleus, precessing at the nuclear Larmor frequency, relaxes through absorption of energy by the spin system, which resonates at the much higher electronic Larmor frequency. If the absorption by the spin system is not perfectly Lorentzian, the relaxation rate extrapolated from an electronic relaxation rate calculated near the center of the resonance may be quite different from that actually observed at the nuclear frequency. From the curves in Figure 3, it is clear that the simultaneous fit produces poor fits to the EPR data. Independent fits of the EPR data are not, however, a great deal better, particularly for the macrocyclic complexes. Thus, while there are undoubtedly problems of incompatability of the NMR and EPR data, much of the poor quality of the fits to the EPR data is due to the inadequacy of the theory used to describe the dominant zero-field splitting relaxation mechanism. The relaxation matrix treatment that led to this theory[7] predicts that the EPR line shape should be a superposition of four Lorentzian lines that, at least at the highest field used, should have very different relaxation rates. No evidence for this is found experimentally: the four transitions appear to be mixed in some way to give a single, approximately Lorentzian line. We have taken the approach of assuming that the relaxation is described by a mean relaxation time. While this gives a much improved description of the field dependence of the relaxation rates, compared to that predicted by the usual McLachlan treatment,[7,28] a more sophisticated treatment of the relaxation rates would no doubt explain the remaining discrepancies. Nonetheless, we believe that our simultaneous least-squares fit gives the best determination of the parameters τ_v^{298}, E_v, and Δ^2 within the limitations of current theory. The values of the correlation time for modulation of the zero-field splitting interaction, τ_v^{298}, are all several times shorter than the rotational correlation times, τ_R^{298}. This suggests that the zero-field splitting interaction is modulated not by rotation of the complex but by random distortions of the coordination sphere. Indeed, a recent molecular dynamics simulation of the $[Yb(H_2O)_8]^{3+}$ ion in solution showed a random pseudorotation, corresponding to sudden 90° jumps of the main axis of symmetry of the square antiprism formed by the eight coordinated water molecules,[45] on a time scale of 11 ps i.e. close to

(43) Frey, S. T.; Chang, C. A.; Carvalho, J. F.; Varadarajan, A.; Schultz, L. M.; Pounds, K. L.; Horrocks, D. W. *Inorg. Chem.* **1993**, *33*, 2882.
(44) Koenig, S. H. *J. Magn. Reson.* **1982**, *47*, 441.
(45) Kowall, T.; Foglia, F.; Helm, L.; Merbach, A. E. *J. Phys. Chem.* **1995**, *99*, 13078.

the τ_v^{298} obtained for $[Gd(H_2O)_8]^{3+}$. If the interaction is modulated by random distortions, this implies that the mean-square zero-field splitting energy, Δ^2, corresponds to a transient zero-field splitting. The three macrocyclic complexes have low Δ^2 values compared to the other complexes. This results in slower electronic relaxation rates in the low field limit, and can be advantageous to their relaxivity properties. This suggests that the instantaneous structure of the macrocyclic complexes is more symmetric than those of the other complexes. On the other hand, the τ_v^{298} values are similar for all the complexes, so that the macrocyclic complexes can change their distortion axis as quickly as the other complexes.

The spin rotation mechanism was invoked in order to explain the slower than expected decrease of $1/T_{1e}$ with magnetic field implied by the ^{17}O NMR relaxation data. The values obtained for the mean-square deviation of the g-tensor, δg_L^2, are quite reasonable compared to those found for Cu^{2+} complexes,[46] and there is no reason why a spin-rotation relaxation mechanism should not operate. In principle, the δg_L^2 values are a measure of the degree of permanent distortion of the complexes. However, we do not attach any significance to the variation of δg_L^2 from one complex to another as it is certainly affected by inadequacies in the description of the electronic relaxation rates due to the zero-field splitting interaction.

Rotation. The rotational correlation times, τ_R^{298}, in Table 4 are reasonably well correlated with the size of the molecules, increasing from the aqua ion to the monomeric complexes to the dimeric complexes. For the dimeric complexes we have distinguished between the rotational correlation time of the Gd^{3+}−water vector, τ_R, and that of the Gd^{3+}−Gd^{3+} vector, τ_{Re}, the former being determined primarily by the NMR and NMRD data and the latter by the electronic relaxation rates. For the $[pip\{Gd(DO3A)(H_2O)\}_2]$ complex the values of τ_R^{298} and τ_{Re}^{298} are identical within error. This implies that the Gd^{3+}−water vector turns as the whole complex turns. For $[bisoxa\{Gd(DO3A)(H_2O)\}_2]$, on the other hand, the value of τ_R^{298} is significantly lower than both the value of τ_{Re}^{298} and the value of τ_R^{298} for $[pip\{Gd(DO3A)(H_2O)\}_2]$. The values of τ_{Re}^{298} are very similar for the two dimeric complexes, as would be expected from their similar size. These facts indicate that the Gd^{3+}−water vector in $[bisoxa\{Gd(DO3A)(H_2O)\}_2]$ rotates more rapidly than the whole complex, implying that either macrocyclic moiety of the complex can rotate independently of the other. This can be interpreted as being due to the more flexible linkage between the two macrocyclic chelating moieties in the bisoxa$(DO3A)_2^{6-}$ compared to the pip$(DO3A)_2^{6-}$ ligand, which is reasonable in the light of the rigidity of the cyclic bridging moiety linked to the planar amide groups. The result of this relatively fast rotation of the Gd^{3+}−water vector is a somewhat lower relaxivity for $[bisoxa\{Gd(DO3A)(H_2O)\}_2]$ than for $[pip\{Gd(DO3A)(H_2O)\}_2]$. It is clear that, in the design of new macromolecular contrast agents, the link between the different chelating groups must be sufficiently rigid that the Gd^{3+}−water vector rotates with the whole complex, if the full relaxivity gains due to slower rotation of the complex are to be achieved.

Diffusion. The diffusion coefficients, D_{GdH}, and activation energies, E_{DGdH}, for the relative motion of water protons and Gd^{3+} complexes, determined primarily from the NMRD measurements, are similar for all the complexes studied. Since the complexes themselves are of different bulk, and so should diffuse at different rates, the similarity of the diffusion coefficients indicates that they are dominated by the much more rapid diffusion of water protons (essentially water molecules). The values obtained are all close to those for self-diffusion of water molecules in pure water: $D^{298} = 2.3 \times 10^{-9}$ m^2 s^{-1} and $E_a = 17.3$ kJ mol^{-1}.[47] This suggests that, while NMRD may not be the ideal method of determining diffusion coefficients, the breakdown of the analysis into inner- and outer-sphere contributions is reliable in this simultaneous data analysis.

The parameters describing the diffusion of one complex with respect to another, D_{GdGd}^{298} and E_{DGdGd}, were obtained from the analysis of the variable-concentration high-field EPR data. The theory applied is certainly only approximate, since the electronic relaxation acts as a correlation time in the intermolecular dipole−dipole relaxation mechanism, so that we do not wish to attach too much importance to the absolute values. Nevertheless, the values obtained are quite reasonable, all being considerably lower than the self-diffusion coefficient of water (see above). We believe that the relatively low values obtained for the two dimeric complexes are significant, and are another manifestation of the increased bulk of the complexes slowing down their motion.

Water Exchange Kinetics. The picture of water exchange on lanthanide(III) complexes that we have built up over a series of publications[4,9,10,22,23,41,46,48−53] is intimately related to the coordination of the complexes in solution. The coordination number of the lanthanide(III) aqua ions is known to change from 9 for the early members of the series to eight for the late members, as a result of the lanthanide contraction.[23,50] The members near the middle of the series exhibit a coordination equilibrium between the octaaqua and enneaaqua complexes: the apparent coordination number of Sm^{3+} is known to be 8.5 from neutron diffraction measurements.[23] The exchange rates for the late lanthanides from Yb^{3+} to Gd^{3+} increase toward the middle of the lanthanide series,[52] while the negative activation volumes indicate an associatively activated exchange mechanism for all octaaqua ions.[41] The increase in exchange rates toward the center of the lanthanide series is interpreted as being due to the relative stabilization of the 9-coordinate transition state as the size of the lanthanide(III) ion increases.

The five contrast agents studied here are, on the other hand, all nine-coordinate Gd^{3+} complexes. The positive activation volumes demonstrate that the exchange mechanism is dissociatively activated, i.e. the transition state in the exchange process resembles an eight-coordinate species. For the monomeric species, there is a considerable amount of evidence that the lanthanide analogues are nine-coordinate across the whole series. This is an indication that the eight-coordinate species, which are the transition states in the exchange processes, are energetically very unfavorable compared to the nine-coordinate ground state, leading to the slow exchange rates compared to the octaaqua ion. This picture of the exchange process has been corroborated by recent measurements of the water exchange rates and activation volumes for the DTPA-BMA^{3-} complexes with Nd^{3+}, Eu^{3+}, Gd^{3+}, Tb^{3+}, Dy^{3+}, and Ho^{3+}.[48] The activation volumes from $[Eu(DTPA\text{-}BMA)(H_2O)]$ to $[Ho(DTPA\text{-}BMA)(H_2O)]$ are all large and positive (between +7.3 and +9.8 cm^3 mol^{-1}), indicating a limiting dissociative D mechanism. The exchange rates increase along the series from [Gd(DTPA-

(46) Poupko, R.; Luz, Z. *J. Phys. Chem.* **1972**, *57*, 3311.
(47) Mills, R. *J. Phys. Chem.* **1973**, *77*, 685−688.
(48) Pubanz, D.; González, G.; Powell, D. H.; Merbach, A. E. *Inorg. Chem.* **1995**, *34*, 4447.
(49) Graeppi, N.; Powell, D. H.; Laurenczy, G.; Zékány, L.; Merbach, A. E. *Inorg. Chim. Acta* **1995**, *235*, 311.
(50) Kowall, T.; Foglia, F.; Merbach A. E. *J. Am. Chem. Soc.* **1995**, *117*, 3790.
(51) Kowall, T.; Foglia, F.; Helm, L.; Merbach A. E. *Chem. Eur. J.* **1996**, *2*, 285.
(52) Cossy, C.; Helm, L.; Merbach, A. E. *Inorg. Chem.* **1988**, *27*, 1973.
(53) Powell, D. H.; Merbach, A. E. *Magn. Reson. Chem.* **1994**, *32*, 739.

BMA)(H_2O)] to [Ho(DTPA-BMA)(H_2O)], consistent with the increased accessibility of the eight-coordinate transition state as the size of the lanthanide(III) ion decreases. Between [Nd(DTPA-BMA)(H_2O)] and [Gd(DTPA-BMA)(H_2O)] the exchange rates vary very little. The activation volume for [Nd(DTPA-BMA)(H_2O)] is near zero (-0.8 ± 1.6 cm^3 mol^{-1}), indicating that as the dissociative mechanism becomes slower, and the lanthanide(III) ion becomes larger, an interchange mechanism (with significant participation from the incoming water molecule) takes over. The interpretation of the phenomenon has been that the crowding of the water binding site determines the rate and mechanism of the water exchange reaction.

On changing from [Gd(DTPA-BMA)(H_2O)] to [Gd(DTPA)(H_2O)]$^{2-}$ two amide ligating groups are replaced by more strongly ligating carboxylate groups. These more strongly coordinating groups can be expected to pull the ligand more tightly around the metal center, thus increasing the crowding at the water binding site. This would favor the dissociative exchange mechanism (indicated by the large positive activation volume) giving the observed increase of water exchange rate (Table 4). Similarly on changing from [Gd(DOTA)(H_2O)]$^-$ to [bisoxa{Gd(DO3A)(H_2O)}$_2$] or [pip{Gd(DO3A)(H_2O)}$_2$] there is a decrease in the number of carboxylate ligands, so that the ligand is pulled less tightly around the metal center and there is less crowding around the water binding site. The dissociative exchange mechanism is thus disfavored leading to the near-zero activation volume for [bisoxa{Gd(DO3A)(H_2O)}$_2$] (see Figure 4) and the relatively low exchange rates for the two dimeric complexes (Table 4). All these results indicate that the best strategy for increasing water exchange rates on Gd^{3+} complexes for use as contrast agents is to increase the crowding at the water binding site and so favor the dissociative exchange mechanism, and that one way to achieve this may be to modify the strength of the ligating groups.

The rather slow water exchange rates for the two dimeric complexes can be expected to have an effect on their proton relaxivities. As a consequence of their longer rotational correlation times there is a gain in relaxivity at the usual imaging fields (20 MHz) of nearly 50% for [pip{Gd(DO3A)(H_2O)}$_2$] and 25% for [bisoxa{Gd(DO3A)(H_2O)}$_2$] with respect to [Gd(DOTA)(H_2O)]$^-$. Simulating an NMRD profile for [bisoxa{Gd(DO3A)(H_2O)}$_2$] with an exchange rate ten times smaller (1.5×10^5 s^{-1}) than that measured and all other parameters unchanged reduced the proton relaxivity to that of [Gd(DOTA)(H_2O)]$^-$, while the same process with an exchange rate ten times greater (1.5×10^7 s^{-1}) enhanced relaxivity at fields lower than the first dispersion, but left the value at 20 MHz nearly unchanged. Similar calculations can be done with [bisoxa{Gd(DO3A)(H_2O)}$_2$] with qualitatively the same result. So, for these dimeric contrast agents, the water exchange rate has a marginal limiting effect on relaxivity at imaging fields (20 MHz). Although the effect is very small for the dimeric complexes presented here, it will become extremely important for higher molecular weight, polymeric contrast agents. If the full gain in relaxivity expected due to the lengthened rotational correlation time is to be achieved, the water exchange rate needs to be *at least* an order of magnitude faster than for the two dimers studied here. Since the water exchange rates in the two dimers are so similar, it would seem that the water exchange rate is determined primarily by the structure of the first coordination sphere of Gd^{3+} and is independent of the structure of the bridging moiety. We thus expect little marketable gain in relaxivity if the same basic coordinating groups are used in the synthesis of polymeric contrast agents.

Conclusions. We have shown that a simultaneous treatment of EPR, ^{17}O NMR, and NMRD data leads to improved definition of the many parameters affecting the proton relaxivity of Gd^{3+} complexes. In addition, we have used high-field EPR data to demonstrate two electron relaxation mechanisms that have not previously been reported for Gd^{3+}, one of which is peculiar to dimeric complexes containing two paramagnetic centers. Our results show that in the design of new polymeric Gd^{3+} complexes, in order to maximize the relaxivity gain, care must be taken that (a) the linking group is sufficiently rigid to ensure that the Gd^{3+}−water vector does not rotate more rapidly than the whole complex and (b) the water exchange rate on the complexes is sufficiently rapid to ensure efficient transfer of relaxivity to the surrounding water.

Our results suggest that potential complexing and linking groups should be screened by studying dimeric complexes, before the time-consuming synthesis of large polymeric species is embarked upon. In addition, it appears that changing the steric crowding at the water binding site through minor modification of ligand structure could be sufficient to ensure that the complexes achieve the second of the above conditions.

Acknowledgment. We thank Nycomed, USA, for providing all the ligands used, for NMRD data, and for their financial support. We are indebted to Silvio Aime *et al.* for the communication of NMRD data on [Gd(DOTA)(H_2O)]$^-$ prior to publication.[37] This work was financially supported by the Swiss National Science Foundation (Grant No. 45419.95) and the Swiss OFES as part of the European COST D1 action.

Supporting Information Available: Reduced transverse and longitudinal ^{17}O relaxation rates and reduced angular frequencies of solutions containing [Gd(H_2O)$_8$]$^{3+}$ (Table S1a−e), [Gd(DTPA)(H_2O)]$^{2-}$ (Table S2a−e), [Gd(DTPA-BMA)(H_2O)] (Table S3a−e), [Gd(DOTA)(H_2O)]$^-$ (Table S4a−j), [pip{Gd(DO3A)(H_2O)}$_2$] (Table S5a−e), and [bisoxa{Gd(DO3A)(H_2O)}$_2$] (Table S6a−f) at 1.4 (a), 4.7 (b), and 9.4 T (c) and transverse electronic relaxation rates at X-band, Q-band, and 2mm band (d) as a function of temperature, proton relaxivities in saline buffer at different temperatures as a function of magnetic field (expressed as proton resonance frequency) (e−j for [Gd(DOTA)(H_2O)]$^-$, e for all others), and reduced transverse ^{17}O relaxation rates of a solution containing [bisoxa{Gd(DO3A)(H_2O)}$_2$] at 9.4 T and 272 K as a function of pressure (Table S6f) (16 pages). See any current masthead page for ordering and Internet access instructions.

JA961743G